

Syntheses and Biological Activities of a Novel Group of Steroidal Derived Inhibitors for Human CDC25A Protein Phosphatase¹

Hairuo Peng,^{‡,†} Wenge Xie,[‡] Diane M. Otterness,[§] John P. Cogswell,^{||} Randy T. McConnell,^{||} H. Luke Carter,^{||} Garth Powis,[‡] Robert T. Abraham,[§] and Leon H. Zalkow^{*,‡}

School of Chemistry and Biochemistry, Georgia Institute of Technology, Atlanta, Georgia 30332, Department of Pharmacology and Cancer Biology, Duke University Medical Center, Durham, North Carolina 27710, Department of Functional Genetics, GlaxoWellcome Inc., Research Triangle Park, North Carolina 27709, and Arizona Cancer Center, University of Arizona, 1515 North Campbell Avenue, Tucson, Arizona 85724-5024

Received October 10, 2000

Silica gel supported pyrolysis of an azido-homo-oxa steroid led to rearrangement, presumably by a mechanism similar to that of solution phase Schmidt fragmentation, to produce a group of novel inhibitors for the oncogenic cell cycle regulator Cdc25A phosphatase. Cyano-containing acid **17**, one of the best inhibitors in this group, inhibited the activity of Cdc25A protein phosphatase reversibly and noncompetitively with an IC₅₀ value of 2.2 μM. Structure–activity relationships revealed that a phosphate surrogate such as a carboxyl or a xanthate group is required for inhibitory activity, and a hydrophobic alkyl chain, such as the cholesteryl side chain, contributes greatly to the potency. Without the cyano group, acid **26** and xanthate **27** were found to be more selective over Cdc25A (IC₅₀ = 5.1 μM and 1.1 μM, respectively) than toward CD45 (IC₅₀ > 100 μM, in each case), a receptor protein tyrosine phosphatase. Several of these inhibitors showed antiproliferative activities in the NCI 60-human tumor cell line screen. These steroidal derived Cdc25 inhibitors provide unique leads for the development of dual-specificity protein phosphatase inhibitors.

Introduction

Reversible phosphorylations of proteins are frequently used in eukaryotic cells as convenient molecular switches for the control of intracellular signaling events. The attachment or removal of phosphate groups from intracellular signaling proteins coordinates the relay of signals to the next level by modulating the formation of protein–protein interactions or by directly regulating the enzyme activities via blocking or unmasking the catalytic site.^{2a} Two types of enzymes regulate protein phosphorylation states: protein kinases, which catalyze the covalent attachment of a phosphate group to the amino acid side chain of a protein, and protein phosphatases, which reverse the procedure.

Eukaryotic protein phosphatases are represented by two distinct families: protein serine/threonine phosphatases (PSTPase), which dephosphorylate phosphoserine (pSer) and phosphothreonine (pThr) in a single-step reaction using a metal-activated water molecule, and protein tyrosine phosphatases (PTPase) which dephosphorylate phosphotyrosine (pTyr) via a two-step reaction involving a cysteinyl-phosphate enzyme intermediate. Dual-specificity protein phosphatases (DSPase) which dephosphorylate both pTyr and pThr residues are considered as a subfamily of PTPase, because they possess the conserved PTPase signature motif HCxxxxR

and employ a similar catalytic mechanism.² Cdc25 cell cycle regulators are examples of DSPases which dephosphorylate contiguous pTyr and pThr on the cyclin dependent kinases (cdks) and have been shown to play crucial roles in cell proliferation.

In human cells, Cdc25 consists of three phase-specific isoforms termed Cdc25A, Cdc25B, and Cdc25C. Both Cdc25C and Cdc25B are considered as regulators of G₂/M transition,³ and Cdc25C was recently found to be a downstream effector of the radiation induced G₂ check point.⁴ In contrast, Cdc25A is expressed early in the G₁ phase and is responsible for the G₁/S transition of cell cycle.⁵ This DSPase dephosphorylates the cdk at Tyr-15 and Thr-14, near the ATP-binding site, allowing binding of ATP to the cyclin/cdk complex and rendering the complex catalytically active to phosphorylate downstream components that initiate DNA synthesis. The dephosphorylation of cyclin/cdk complexes by Cdc25 phosphatases is tightly regulated in normal cells. However, accumulating evidence suggests that inappropriate amplification or activation of Cdc25A or Cdc25B is characteristic of a number of human cancers, including breast cancers.⁶ Enforced expression of Cdc25A or B causes cellular transformation, and the transcription and catalytic activities of both proteins are directly regulated by two other protooncogenes products, c-Myc and c-Raf, respectively.⁷ Thus, deregulation of Cdc25A and Cdc25B activities, either through overexpression or abnormal activation, may contribute to the growth of certain types of cancer. Therefore, small molecule inhibitors of these two enzymes may possess novel antitumor activities.⁸

In contrast to PSPTase, for which a number of very potent inhibitors, such as Okadaic acid (IC₅₀ = 49 nM,

* To whom correspondence should be directed: Prof. Leon H. Zalkow, School of Chemistry and Biochemistry, Georgia Institute of Technology, Atlanta, GA 30332-0400. Phone: (404) 894 4045. Fax: (404) 894 7452. E-mail:leon.zalkow@chemistry.gatech.edu.

[‡] Georgia Institute of Technology.

[§] Duke University Medical Center.

^{||} GlaxoWellcome Inc.

[†] University of Arizona.

[†] Current address: Yale University, Department of Chemistry, P.O. Box 208107, New Haven, CT 06520-8107.

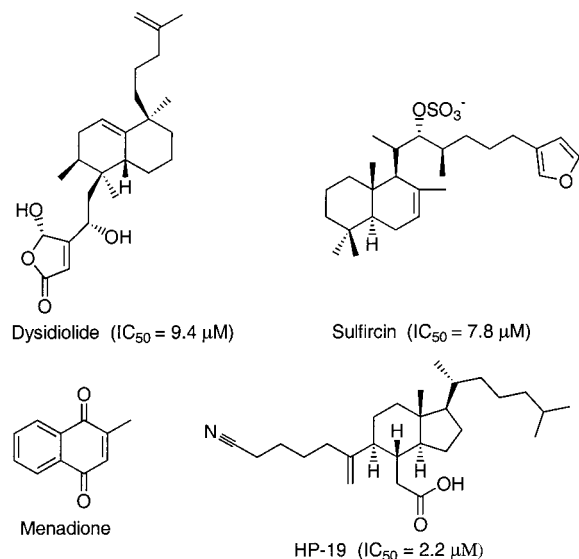


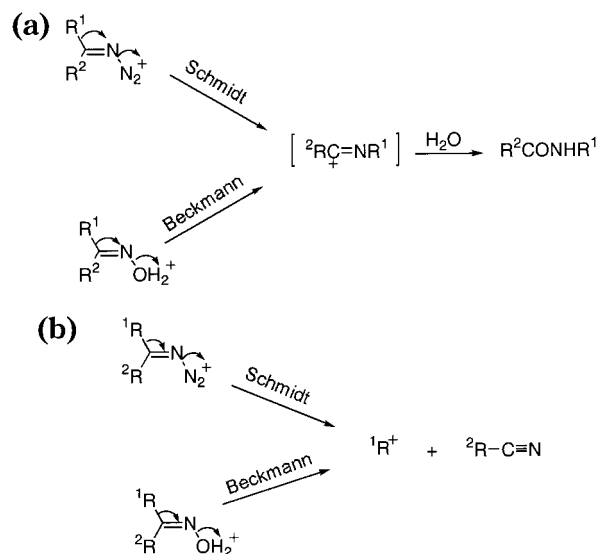
Figure 1. Chemical structures of dysidiolide, sulfircin, menadione, and HP-19.

PP1),⁹ have been reported, the development of inhibitors for PTPase, particularly for its DSPase subfamily, have just recently attracted intense effort. Not long ago, a broad-spectrum protein phosphatase inhibitor, sodium othrovanadate,¹⁰ was the only readily available Cdc25 phosphatase inhibitor widely used. Later, a few small molecule Cdc25A phosphatase inhibitors were reported, including natural products dysidiolide (IC₅₀ = 9.4 μM,^{11a} *p*NPP; IC₅₀ > 50 μM, mFP^{11b}), sulfircin (IC₅₀ = 7.8 μM, *p*NPP),¹² and menadione (vitamin K₃) and its naphthoquinone analogues,¹³ which inactivate Cdc25A irreversibly by forming Michael adducts (Figure 1). A combinatorial library of inhibitors based on the pharmacophore of Ser/Thr phosphatase resulted in competitive Cdc25A inhibitors such as SC-ααδ9 (IC₅₀ = 15 μM, FDP; IC₅₀ = 4 μM, *p*NPP).¹⁴ Libraries of dipeptidyl phosphonates and malonates resulted in several noncompetitive Cdc25A inhibitors.¹⁵ We have also recently reported steroidal derived acids as Cdc25A inhibitors.^{1,22}

We initiated a program of designing novel Cdc25A inhibitors based on templates of readily available natural products. The rigidity and well-defined stereochemistry of the cholesteryl template makes it a good scaffold for distal functionalization. It has been suggested that, in dysidiolide, the γ -hydroxybutenolide moiety likely serves as a surrogate phosphate, while the long side chain occupies a hydrophobic binding pocket near the active site. We visualized that the C and D rings and the attached C8 side chain of cholesteryl acetate could mimic the hydrophobic rings, with attendant side chains, of dysidiolide, and the surrogate phosphate could be constructed from the A and B rings of the cholesteryl template via some type of fragmentation reaction of these rings. The C-3 acetoxy group and C-5 double bond of cholesteryl acetate would obviously serve as entries in this approach.

Herein we report the discovery of a group of novel Cdc25A inhibitors synthesized by pyrolysis of a readily available natural product derivative, 3 α -azido-B-homo-6-oxa-4-cholesten-7-one (**3**), on silica gel (Scheme 2). HP-19 (**17**), one of the best inhibitors in this series, inhibited the dephosphorylation of fluorescein diphosphate by Cdc25A with an IC₅₀ of 2.2 μM (Table 4). These

Scheme 1. Schmidt and Beckmann (a) Rearrangement and (b) Fragmentation

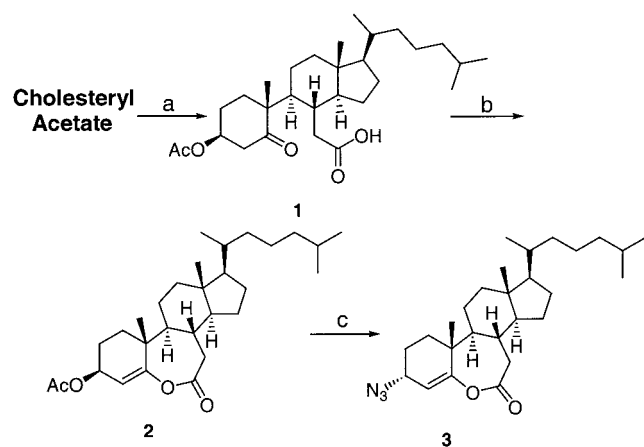


inhibitors showed antiproliferative activities in the NCI 60-human tumor cell line screen. On the basis of an analysis of structure–activity-relationships, a group of more potent Cdc25A inhibitors of simpler structures were synthesized; the best one (**34**) showed IC₅₀ value of 0.7 μM (Table 9).

Results and Discussion

Chemistry. The Beckmann and Schmidt rearrangements are classical examples of molecular rearrangements in which an alkyl or aryl group migrates with their bonding electrons to adjacent electron-deficient nitrogen atoms to form amides or lactams. (Scheme 1a). However, if cleavage of the adjacent C–C bond leads to the formation of a carbonium ion with considerable stability, fragmentation reactions may occur resulting in a nitrile and a positively charged fragment.¹⁶ These types of fragmentation reactions have been referred to as “abnormal”, “second order” Beckmann and Schmidt rearrangements, or Beckmann and Schmidt fragmentations (Scheme 1b).¹⁷ Examples of these two types of fragmentation reactions have been reported to yield nitriles, and carbocations that eventually formed double bonds, under Beckmann¹⁹ or Schmidt¹⁸ rearrangement conditions. We decided to take advantage of this type of fragmentation reaction to cleave the A and B rings of the cholesteryl template to obtain favorable pharmacophores for Cdc25A inhibition: an α,β -unsaturated cyano group which is an excellent substrate for Michael addition by the cysteine group in the active site, and a carboxylic acid group that may coordinate with the active site arginine.

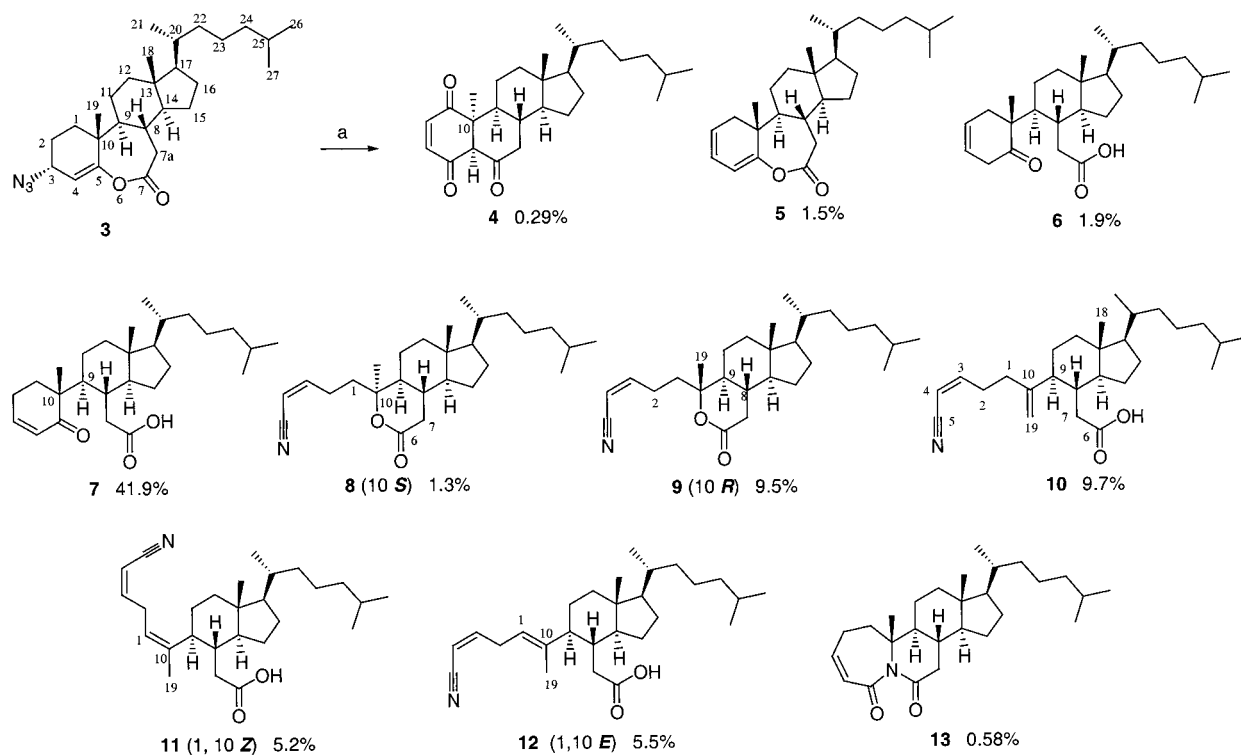
For unknown reasons, the Schmidt fragmentation (Figure 1b) of 5,6-seco-3-cholesten-6-oic acid (**7**) in solution was unsuccessful. Therefore, compound **3** was synthesized as a promising precursor. As illustrated in Scheme 2, pyrolysis precursor **3** was prepared by ozonolysis of cholesteryl acetate,²⁰ followed by conversion of the resulting keto acid **1** to 3 β -acetoxy-B-homo-6-oxa-4-cholesten-7-one (**2**) with thionyl chloride at room temperature. Exposure of **2** to sodium azide (10% aqueous) at room temperature gave **3** quantitatively.

Scheme 2^a

^a (a) O₃, -60 °C, hexane, 45 min; piperidine, 0 °C, 3 h; 2 M HCl; (b) SOCl₂, CH₂Cl₂, 2 h; (c) 2 equiv of NaN₃/H₂O (10%), acetone, 2 h.

However, attempts to rearrange this compound in different solvents at temperatures up to 160 °C were unsuccessful, as well. Fragmentation of the A and B rings of the cholesteryl template was eventually accomplished by pyrolyzing 3 α -azido-B-homo-6-oxa-4-cholesten-7-one (**3**) on silica gel. Silica gel (0.040–0.063 mm; EM science) was evenly coated with **3** to give 20 wt % solid, after evaporation of the solvent. Pyrolysis of this solid at 180 °C for 1 h, followed by extraction, silica gel column chromatography, and reverse phase HPLC, gave products **4–13** (Scheme 3) with diverse structural features.

Formation of compounds **5–7** is seen to readily arise through elimination of the azido group, and further opening of the lactone B ring leads to **6** and **7**. Compounds **8–12**, the fragmentation products, and **13** may

Scheme 3^a

^a (a) Compound **3** was coated on silica gel to give a 20% weight solid and pyrolyzed at 180 °C for 1 h.

arise from a common fragmentation intermediate. As illustrated in Schemes 4 and 5, compounds **8–13** can be visualized as arising from the common carbocation intermediate **C**. Heating of the pyrolysis precursor **3** on silica gel would lead to **A** by a 3,3-sigmatropic rearrangement and protonation. Fragmentation of **A** would be initiated by opening of the B ring to give **B** that already contains a favorable carboxyl group necessary for Cdc25A inhibition. Intermediate **B** can be seen to possess an ideal structure to undergo the Schmidt fragmentation reaction: cleavage of the C-5, C-10 bond leads to a stable tertiary carbocation. As a result, loss of nitrogen gives an α,β -unsaturated cyano group and a stable carbocation at C-10 in the common intermediate **C** for the formation of compounds **8–13**.

As shown in Scheme 4, trapping of the carbocation by lone pair electrons on the carboxyl oxygen would give rise to epimeric lactones **8** and **9**, while elimination of hydrogen atoms from adjacent carbons would result in unsaturated isomers, **10–12**. As illustrated in Scheme 5, recombination of the carbocation and the cyano group in **C** followed by hydrolysis through a Ritter reaction²¹ would give iminol **D**, which upon reaction with the B ring carboxyl group and loss of water, would result in the formation of imide **13**.

Another compound (**4**) of unexpected structure was formed in the same pyrolysis reaction. Compound **4** (Figure 2) contains a dihydro-quinone moiety, and surprisingly, the stereochemistry at C-10 has been inverted as compared to the cholesteryl acetate starting material. It was reasoned that this compound might be formed from one of the major products of the pyrolysis reaction, compound **7**, by rotation of the C₁₀–C₉ bond, oxidation of the enone, and finally cyclization and loss of water as seen in Scheme 6.

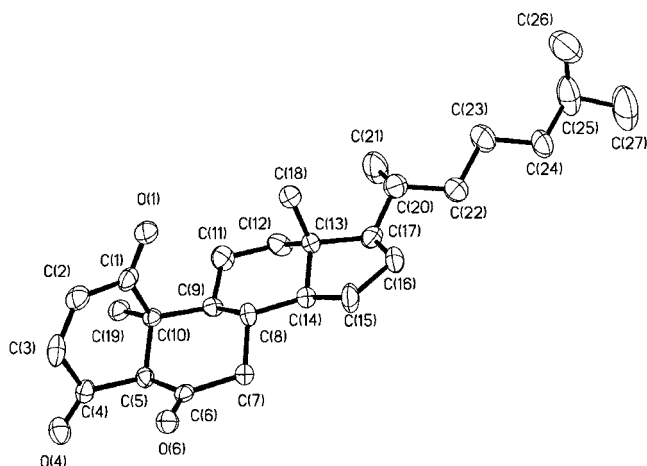
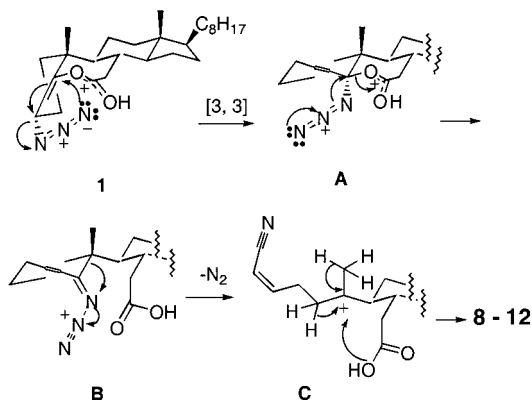
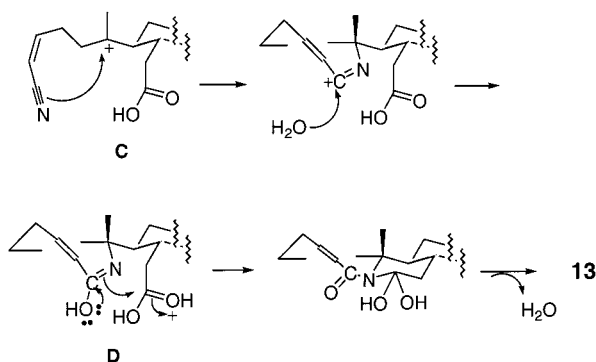


Figure 2. ORTEP drawing of the X-ray structure for compound **4**.

Scheme 4. Proposed Mechanism for the Formation of Compounds **8–12**



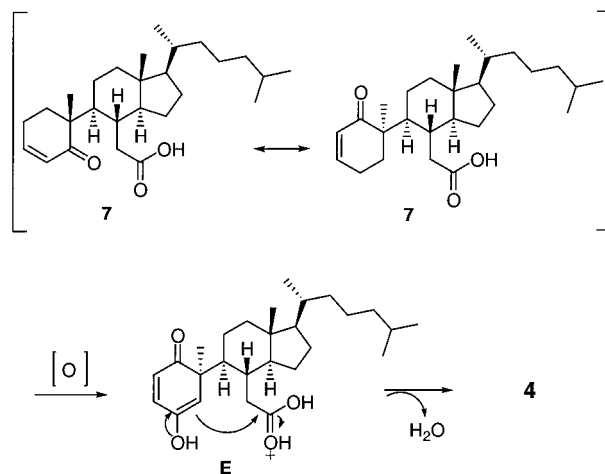
Scheme 5. Proposed Mechanism for the Formation of Compound **13**



Compound **5** was hydrogenated to remove the Δ^3 double bond to give **14**. Compounds **7** and **9–13** were hydrogenated to remove the conjugated double bonds using 10% Pd/C to give compounds **15–20**, respectively. Compound **10** (Scheme 3) was hydrogenated using 5% Pt/C to saturate both double bonds to yield C-10 epimers **21** and **22**.

As shown in Scheme 7, base-catalyzed hydrolysis of lactone **9** in methanol gave tetrahydrofuran **23**, presumably formed by Michael addition of the C-10 oxygen to the conjugated cyano group. Michael addition of the solvent, methanol, at the same position gave compound **24**. Similarly, base-catalyzed solvolysis of compound **10** in ethanol gave **25**. When the conjugated double bond

Scheme 6. Proposed Mechanism for the Formation of Compound **4**

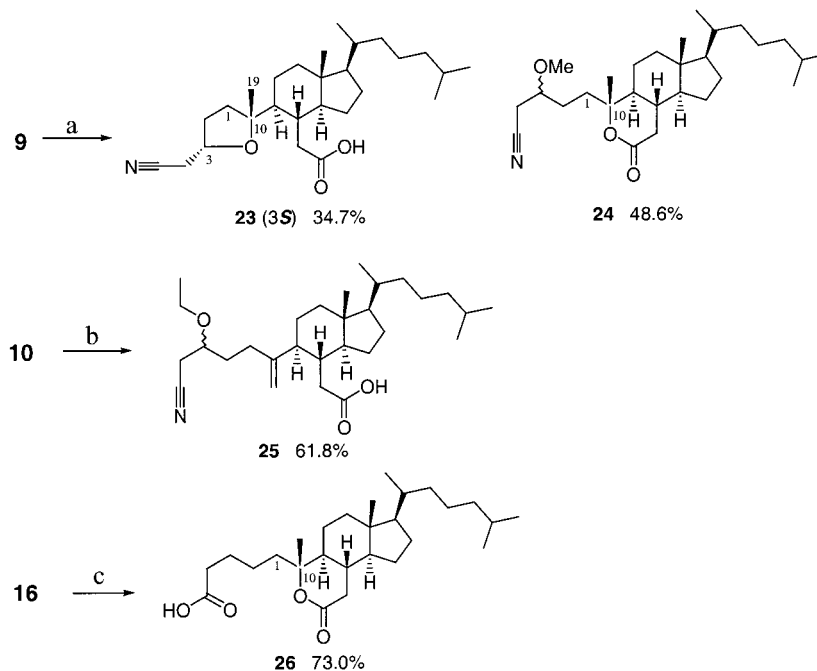


was removed to eliminate the possibility of Michael addition, as in compound **16**, the cyano group was hydrolyzed into a carboxyl group to give compound **26**.

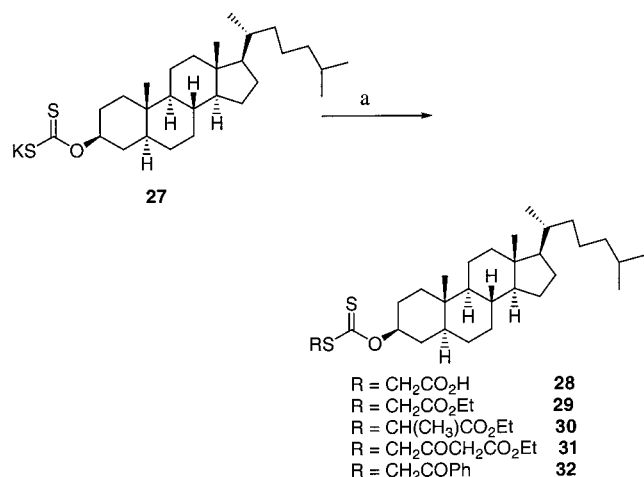
Compounds **28–37** were synthesized as illustrated in Schemes 8–10, in order to introduce other functional groups that might serve as phosphate surrogates. As seen in Scheme 8, cholestanyl xanthates **28–32** were synthesized by treatment of potassium *O*-cholestanyl xanthate (**27**) with 1 equiv of the appropriate alkyl halide in DMSO. Compound **27** was obtained by treatment of the potassium salt of cholesterol with carbon disulfide.²² As shown in Scheme 9, compound **33** was synthesized by reductive amination using cholesterol-3-one and δ -amino butyric acid. Cholestanyl-*O*-acetic acid **34**, cholestanyl thiocarbamates **35** and **36**, and cholestanyl carbamate **37** were synthesized by treatment of cholesterol with sodium hydride followed by reaction with bromo acetic acid, aryl isothiocyanates, and phenyl isocyanate, respectively (Scheme 10).

Spectroscopic Characterization. The products of the pyrolysis reaction exhibited varied functionalities in place of the previous A and B rings of the cholesterol skeleton. Structures of compounds **4**, **8**, and **13** were firmly established through X-ray crystallographic analysis (Figures 2–4). Structures of other compounds were identified by IR, MS, and a series of NMR experiments including ^1H and ^{13}C NMR, DEPT, COSY, HMQC, HMBC, and NOESY. The ^1H and ^{13}C NMR spectral assignments of the characteristic resonances for representative new compounds are listed in Tables 1–3. As seen in Tables 1 and 2, the chemical shifts of the Me-19 protons are the defining features distinguishing the molecules, and the ^{13}C signals of Me-19, with an α configuration, as in compounds **4** and **8**, appear at much higher (δ 26 ppm) resonances than the ones with a β configuration (Table 3).

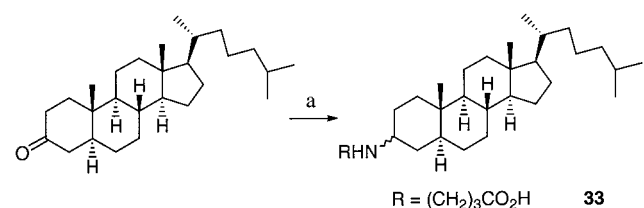
Compounds **8–12** have common structural features with the cholesteryl side chain and C, D rings intact, while the A and B rings have been opened to give chains containing a conjugated cyano group exhibiting absorptions around 2220–2230 cm^{-1} in their IR spectra. Two highly conjugated olefinic protons resonate as a downfield doublet triplet (H-3) and an upfield doublet (H-4) in the ^1H NMR spectra of these compounds, the coupling constants (11.0 Hz) indicating cis-double bonds

Scheme 7. Base-Catalyzed Hydrolysis and Michael Addition of Compounds **9**, **10**, and **16**^a

^a (a) 0.6% NaOH/MeOH, reflux 10 h; 2 M HCl; (b) 6% NaOH/EtOH, reflux 10 h; 2 M HCl; (c) 6% NaOH/MeOH, reflux 10 h; 2 M HCl.

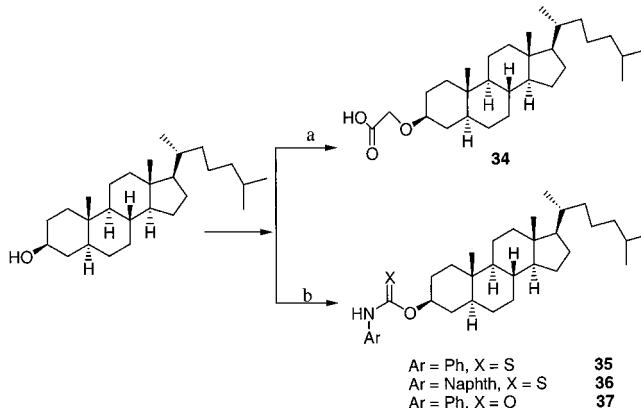
Scheme 8^a

^a Reagents: (a) RX (X = Cl or Br), DMSO, 80–85%.

Scheme 9^a

^a Reagents: (a) δ -amino butyric acid, NaBH₃CN, CH₃OH/THF, 85%.

(Table 1). The C-10 quaternary carbons at δ 86.3 and 86.6 ppm (Table 3) in compounds **8** and **9**, respectively, are indicative of a newly formed stereocenter attached to an oxygen atom. Compounds **8** and **9** were identified as lactone epimers by IR absorptions of a six-membered δ -lactone at 1720 and 1733 cm⁻¹, respectively. The relative stereochemistry of these two isomers were confirmed by the single-crystal X-ray diffraction of **8**,

Scheme 10^a

^a Reagents: (a) NaH, THF, BrCH₂CO₂H, 60%; (b) NaH, THF, ArNCS or ArNCO, 75–80%.

and the NOE observed between Me-19 protons and H-8 (δ 2.07, 1H, m), as well as that between H-2 (δ 2.55, 2H, m) and H-9 (δ 1.49, 1H, m), in the NOESY spectrum of **9**. Compounds **10**–**12** were assigned as carboxylic acids for the characteristic absorptions around 3350–2500 (br) and 1700 cm⁻¹ in the IR spectra. The chemical shifts for the H-1 and Me-19 protons (Table 1) indicated different double bond configurations for compounds **10**–**12**. Compound **11** was assigned as 1,10*Z* based on the NOE observed between H-1 and Me-19 protons while **12** was assigned as 1,10*E* by the NOE between H-2 and Me-19 protons.

The configuration at C-3 in compound **23** (Scheme 7), the product of intramolecular Michael addition of **9**, was determined as *S* by the NOE observed between the signals for Me-19 protons and H-3 (Table 2). Compounds **21** and **22**, the C-10 epimers derived from the hydrogenation of **10** (Scheme 3), exhibit differentiated Me-19 signals at δ 0.89 (d, 3H, *J* = 6.6 Hz) and 0.78 (d, 3H, *J* = 6.6 Hz), respectively. However, without crystal structures for these compounds, it is not possible to assign

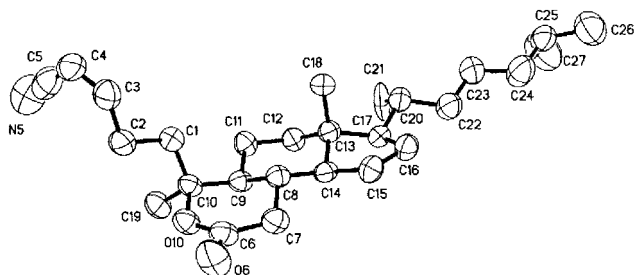
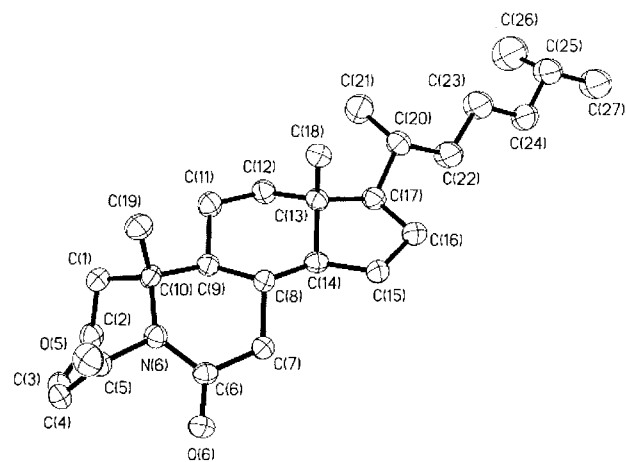
Table 1. ^1H NMR Data for Compounds **8–12**

no.	chemical shift, ppm (CDCl_3)				
	8	9	10	11	12
19	1.43 (s, 3H)	1.34 (s, 3H)	4.93 (s, 1H), 4.84 (s, 1H)	1.67 (s, 3H)	1.60 (s, 3H)
1	1.85 (m, 2H)	1.75 (m, 2H)	2.17 (t, 7.2 Hz, 2H)	5.18 (t, 7.7 Hz, 2H)	5.17 (t, 7.2 Hz, 2H)
2	2.63 (m, 2H)	2.55 (m, 2H)	2.59 (m, 2H)	3.10 (dd, 7.7, 5.5 Hz, 2H)	3.08 (t, 7.2 Hz, 2H)
3	6.54 (dt, 11.0, 7.8 Hz, 1H)	6.52 (dt, 10.8, 7.8 Hz, 1H)	6.50 (dt, 11.0, 7.2 Hz, 1H)	6.37 (dt, 10.9, 7.7 Hz, 1H)	6.38 (dt, 11.1, 7.5 Hz, 1H)
4	5.35 (d, 11.1 Hz, 1H)	5.32 (d, 10.5 Hz, 1H)	5.33 (d, 11.0 Hz, 1H)	5.27 (d, 10.9 Hz, 1H)	5.27 (d, 10.4 Hz, 1H)
7	2.61 (dd, 18.0, 5.1 Hz, 1H)	2.60 (dd, 17.7, 4.8 Hz, 1H)	2.35 (dd, 15.0, 3.3 Hz, 1H)	2.22 (dd, 15.4, 3.3 Hz, 1H)	2.22 (dd, 15.4, 4.4 Hz, 1H)
	2.02 (dd, 18.0, 11.5 Hz, 1H)	2.00 (dd, 17.7, 11.5 Hz, 1H)	2.10 (dd, 15.0, 6.6 Hz, 1H)	2.04 (dd, 15.4, 7.6 Hz, 1H)	2.07 (dd, 15.4, 6.6 Hz, 1H)

Table 2. ^1H NMR Data for Compounds **4, 6, 13,** and **23**

position	chemical shift, ppm (CDCl_3)			
	4	6	13	23
19	1.43 (s, 3H)	1.05 (s, 3H)	1.30 (s, 3H)	1.25 (s, 3H)
1		3.20 (d, 21.1 Hz, 1H)	2.41–2.22 (m, 2H)	NA ^a
2	6.69 (dd, 10.2, 1.5 Hz, 1H) ^b	2.85 (d, 21.1 Hz, 1H)	NA ^a	NA ^a
3	6.50 (d, 10.2 Hz, 1H) ^b	5.68 (m, 1H)	6.74 (ddd, 10.4, 7.7, 2.7 Hz, 1H)	4.20 (m, 1H)
4		2.46 (dd, 17.4, 5.5 Hz, 1H)	6.21 (dd, 10.4, 2.7 Hz, 1H)	2.70–2.44 (m, 2H) NA ^a
		2.00 (buried in, 1H)		
5	3.39 (s, 1H)			
7	NA ^a	2.27 (dd, 16.6, 2.7 Hz, 1H)	2.43 (dd, 17.6, 4.4 Hz, 1H)	2.70–2.44 (m, 2H) NA ^a
		2.09 (dd, 16.6, 7.5 Hz, 1H)	2.00 (dd, 17.6, 12.5 Hz, 1H)	

^a Not assigned. ^b Assignment may be interchanged.

**Figure 3.** ORTEP drawing of the X-ray structure for compound **8**.**Figure 4.** ORTEP drawing of the X-ray structure for compound **13**.

unequivocal absolute configurations at C-10 in these isomers.

Biological Evaluation. The inhibition effects of compounds synthesized were evaluated as inhibitors of human Cdc25A phosphatase at 25 °C using fluorescein diphosphate (FDP) as substrate. Some of the best

Table 3. ^{13}C Data for Compounds **4, 6, 8–10, 13,** and **23**

carbon	chemical shift, ppm (CDCl_3)						
	4	6	8	9	10	13	23
19	26.1	16.8	26.0	18.6	111.2	18.7	21.2
10	55.3	50.9	86.3	86.6	150.2	62.0	89.7
1	201.0 ^b	40.9	NA ^a	NA ^a	32.5	NA ^a	NA ^a
2	140.1	124.4	NA ^a	NA ^a	29.9	NA ^a	NA ^a
3	139.1	126.0	154.4	154.5	154.7	149.6	74.4
4	196.4 ^b	39.1	100.2	99.8	99.8	128.8	NA ^a
5	71.6	217.1	115.8	115.9	116.0	169.3	116.8
6	206.0 ^b	178.9	170.6	170.8	179.1	175.7	174.1

^a Not assigned. ^b Assignment may be interchangeable.

inhibitors were tested for their inhibitory activities against Cdc25A and CD45 receptor protein tyrosine phosphatase²³ using *p*-nitro phenyl phosphate (*p*NPP) as substrate. The results are listed in Tables 4–9.

The orientations of the cyano-containing side chains vary in the double bond isomers **10–12** as seen in the energy minimized conformations (Hyperchem). These differing conformations may account for the differentiated inhibitory activities observed for compounds **10–12** (9.7–36.3 μM , Table 4). Increasing the flexibility of the cyano-containing side chain by saturating the double bonds, as in compounds **17–19** and **21–22**, significantly increased the potencies of these compounds (2.5–1.9 μM , Table 4). Removal of the Δ^3 double bond by Michael addition, as in compound **25**, also resulted in better inhibitory activity (2.9 μM) than the parent compound. However, formation of the tetrahydrofuran ring as in **23** resulted in reduced inhibitory activity (15.8 μM), perhaps, because of the increased rigidity of the compound. Compounds **4** and **13**, although containing the α,β -unsaturated ketone as Michael acceptor, did not show Cdc25A inhibitory activity.

The ready formation of compounds **23** and **25** through base-catalyzed solvolysis illustrated the ease of forma-

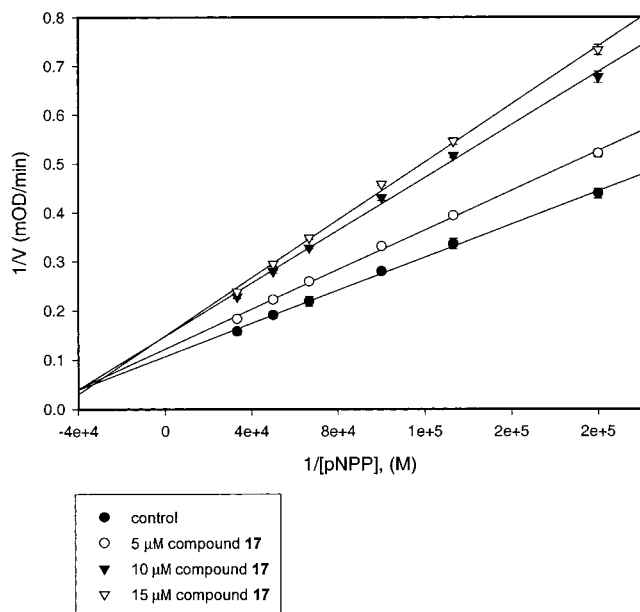


Figure 5. Lineweaver–Burk plot for the CD45 inhibition by compound **17**.

Table 4. Protein Phosphatase Inhibition Activities of Compounds **10–12**, **17–19**, **22–23**, and **25**

compd	R ₁	Δ ³	Δ ^{1,10}	Δ ^{10,19}	config. C ₁₀	Cdc25A ^a IC ₅₀ (μM)	Cdc25A ^b IC ₅₀ (μM)	CD45 ^b IC ₅₀ (μM)
10	-H	cis		present		9.7		
11	-H	cis	Z			36.3		
12	-H	cis	E			24.2		
17	-H			present		2.2	8.3	12.2
18	-H		Z			2.4		
19	-H		E			2.5	9.3	13.2
21	-H					2.2		
22	-H					1.9	9.1	8.6
23	-O-C ₁₀				10R	15.8		
25	-OEt			present		2.9		

^a Assay using fluorescein diphosphate (FDP) as substrate.

^b Assay using *p*-nitro phenyl phosphate (NPP) as substrate.

tion of Michael adducts at the α,β -unsaturated cyano group. However, the observation that elimination of the Michael addition potential, as in compounds **17–19**, **21**, **22**, and **25**, increased inhibitory activity suggests that irreversible binding of these inhibitors to the cysteine group at the active site of Cdc25A is responsible for the observed activity. The reversible inhibition of compound **10** was confirmed by a revised Cdc25A inhibition assay, using Cdc25A bound GST beads. After preincubation with the inhibitor, the enzyme bound beads were washed with assay buffer before starting the phosphatase assay. Results indicated that removal of inhibitor **10** by washing reversed inhibition of the enzyme.

It was unexpected that assays using *p*NPP exhibited higher IC₅₀ values than those obtained with FDP as substrate (Table 4). In the literature,¹⁴ the IC₅₀ reported for SC- $\alpha\alpha$ 9 was higher with FDP (IC₅₀ = 15 μM, FDP; IC₅₀ = 4 μM, *p*NPP). As shown in Table 4, compounds **17**, **19**, and **22** also showed moderate inhibition against

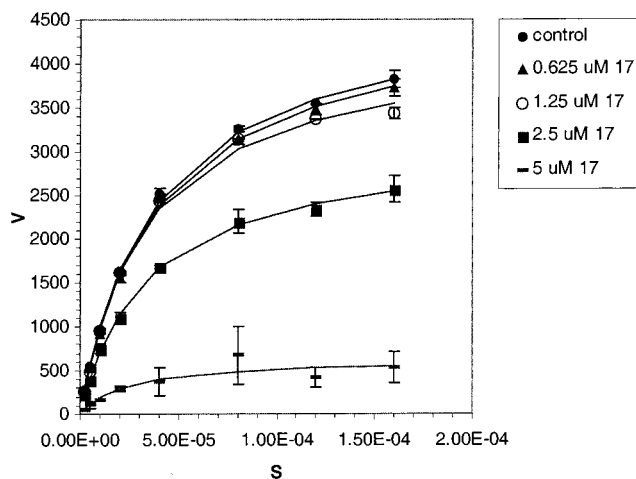


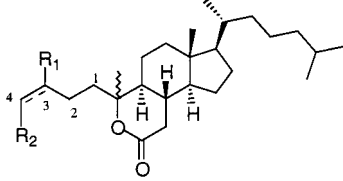
Figure 6. Michaelis–Menten plot for the Cdc25A inhibition by compound **17**.

Table 5. V_{max} and Apparent K_m for Cdc25A Inhibition by Compound **17**

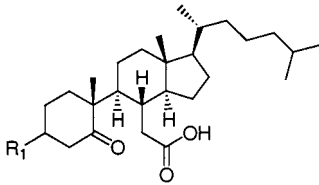
inhibitor concn (μM)	V _{max}	SE (V _{max})	K _m (μM)	SE (K _m)
control	4724	70	37.4	1.6
0.625	4607	84	37.4	1.96
1.25	4261	84	32.3	1.91
2.5	3074	99	33.6	3.24
5	632	141	23.1	17.3

CD45, a receptor tyrosine phosphatase. The kinetic characteristics of CD45 inhibition with compound **17** were studied using *p*NPP as substrate. As shown in Figure 5, the Lineweaver–Burk plot was most consistent with a mixed inhibition model. However, the kinetic characteristics of compound **17** for Cdc25A, using 3-OMe FMP as substrate, exhibited a noncompetitive pattern. Figure 6 shows the Michaelis–Menten plot, and the V_{max} and apparent K_m derived from the plot are listed in Table 5. Compound **17** inhibited the enzyme by decreasing the V_{max}, but the apparent K_m was unchanged within the experimental error. These observations suggest that compounds, like **17**, which contain a cyano group might not bind to Cdc25A or CD45 protein phosphatase specifically at the active site. It is worth noting that simple cholesteryl acid, 3-oxo-4-cholesten-2 β -acetic acid, has been shown to inhibit Cdc25A competitively, suggesting that this type of simple steroidal acid may interact with the arginine group at the substrate binding site.²²

As shown in Table 6, repeated testing of lactone **9** gave an average IC₅₀ value of 29 μM, which is larger than previously reported.¹ This suggested that the carboxyl group in compound **10** and the related compounds was important for inhibitory activity. Lactone **8**, the 10*S* isomer of **9**, is essentially inactive, presumably due to the unfavorable orientation of the cyano-containing side chain. However, when the conjugated double bonds were removed as in derivatives **16** and **24**, the potency increased presumably because of the greater flexibility of the side chains in these inhibitors. Compound **26** (Scheme 7), containing both a carboxyl group and a lactone ring, exhibited a much better IC₅₀ (5.1 μM) compared to compound **9**, suggesting that **26** may orient differently in the enzyme, taking advantage of the free carboxyl group. The fact that compound **26** was

Table 6. Protein Phosphatase Inhibition Activities of Compounds **8**, **9**, **16**, **24**, and **26**


compd	R ₁	R ₂	Δ ³	config. C ₁₀	Cdc25A ^a IC ₅₀ (μM)	Cdc25A ^b IC ₅₀ (μM)	CD45 ^b IC ₅₀ (μM)
8	-H	-CN	present	<i>S</i>	>50		
9	-H	-CN	present	<i>R</i>	29	>100	>100
16	-H	-CN		<i>R</i>	24		
24	-OMe	-CN		<i>R</i>	10.5		
26	-H	-COOH		<i>R</i>	5.1	11.6	>100

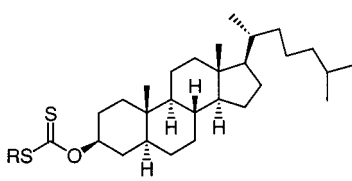
^a Assay using fluorescein diphosphate (FDP) as substrate.^b Assay using *p*-nitro phenyl phosphate (*p*NPP) as substrate.**Table 7.** Cdc25A Inhibitory Activities of Compounds **1**, **6**, **7**, and **14**


compd	R ₁	double bond	Cdc25A ^a IC ₅₀ (μM)
1	-OAc		9.3
6	-H	Δ ²	5.8
7	-H	Δ ³	9.5
15	-H		5.9

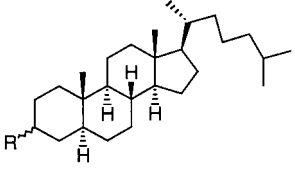
^a Assay using fluorescein diphosphate (FDP) as substrate.

inactive for CD45 (IC₅₀ > 100 μM) makes it a good selective inhibitor for Cdc25A.

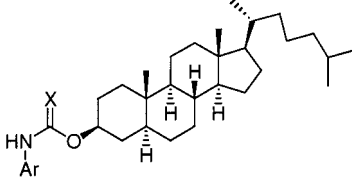
As shown in Table 7, compounds **1**, **6**, **7**, and **14**, which simply contain the carboxyl group and cholesteryl side chain, also showed fairly good inhibitory activities against Cdc25A, demonstrating that the cyano groups in compounds **8–12**, **16–19**, and **21–25** were not essential for inhibition. We have reported, however, a hydrophobic side chain is crucial for inhibitory activity.²² In light of these considerations, a series of cholestanol derivatives (**27–37**) were synthesized to evaluate contributions of alternative phosphate surrogates. As shown in Table 8, compound **27**,²² with the dithiocarboxylic acid group and the cholesteryl side chain, exhibited potent selective inhibitory activity over Cdc25A (IC₅₀ = 1.1 μM, Cdc25A; IC₅₀ > 100 μM, CD45). Addition of an acetic acid group to the xanthate, as in **28**, slightly increased Cdc25A inhibitory activity (IC₅₀ = 0.9 μM). Similarly, addition of an acetic acid group directly to cholestanol resulted in excellent inhibitory activity for compound **34** (IC₅₀ = 0.7 μM, Table 9). However, introduction of an γ -amino butyric acid group to the cholestanol skeleton, as in compound **33**, led to acute loss of activity as compared to compounds **27**, **28**, and **34**. When the dithiocarboxylic acid group or the carboxylic acid group was masked as in compounds **29–32**, activity was completely lost. Unexpectedly, without a free carboxyl group, the *N*-phenyl thiocarbamate derivative of cholestanol (**35**) was a very active Cdc25A inhibitor (IC₅₀ = 2.1 μM), while *N*-naphthyl thiocarbamate **36** and *N*-

Table 8. Protein Phosphatase Inhibitory Activities of Compound **27–32**


compd	R	Cdc25A ^a IC ₅₀ (μM)	Cdc25A ^b IC ₅₀ (μM)	CD45 ^a IC ₅₀ (μM)
27	-H	1.1	11.7	>100
28	-CH ₂ CO ₂ H	0.9		
29	-CH ₂ CO ₂ Et	>100		
30	-CH(CH ₃)CO ₂ Et	>100		
31	-CH ₂ COCH ₂ CO ₂ Et	>100		
32	-CH ₂ COPh	>100		

^a Assay using fluorescein diphosphate (FDP) as substrate.^b Assay using *p*-nitro phenyl phosphate (NPP) as substrate.**Table 9.** Cdc25A Inhibitory Activities of Compounds **33** and **34**


compd	R	config. C ₃	IC ₅₀ (μM)
33	-NH(CH ₂) ₃ CO ₂ H	<i>R, S</i>	16% ^a
34	-OCH ₂ CO ₂ H	<i>S</i>	0.7

^a Percentage inhibition at 11 μM.**Table 10.** Cdc25A Inhibitory Activities of Compounds **35–37**


compd	X	Ar	IC ₅₀ (μM)
35	S	Ph	2.1
36	S	Naphth	19% ^a
37	O	Ph	18% ^a

^a Percentage inhibition at 10 μM.

phenyl carbamate **37** were essentially inactive (Table 10). The mechanism of inhibition for **35** is currently unknown.

The growth inhibition effects of representative Cdc25A inhibitors were tested in the NCI 60 human tumor cell lines representing eight types of solid tumors and leukemia. The cell growth and viability were measured using a protein stain sulforhodamine (SRB), which binds to basic amino acids of proteins in the living cells that remain attached to the culture plate after washing.^{24–25}

Table 11 shows the GI₅₀ values (micromolar concentrations required to produce 50% growth inhibition) of different compounds for sensitive subpanels in the NCI panel. As shown in Table 11, the cyano-containing acids (**17**, **19**, **21**, **22**) that inhibit Cdc25A exhibited similar growth inhibition patterns with mean GI₅₀s (MG-MID) at about 8 μM. Compound **23**, which contains a tetrahydrofuran moiety, in addition to the cyano and carboxyl groups, showed essentially the same growth inhibition

Table 11. Inhibition of in Vitro Cancer Cell Lines by Compounds **9**, **13**, **14**, **16**, **17**, **19**, **21–23**, and **26**

disease type and cell lines	GI ₅₀ (μM) ^a									
	9	13	14	16	17	19	21	22	23	26
non-small cell lung cancer										
A549/ATCC	15.0	4.27	10.8	5.51	5.21	7.33	5.09	4.35	8.25	8.30
NCI-H23	14.8	4.85	19.0	5.63	5.12	7.40	5.27	5.85	5.75	4.92
NCI-H522	0.89	6.10	>25	>25	ND ^c	17.3	>25	>25	0.94	>25
colon cancer										
COLO205	8.49	4.76	>25	4.75	5.10	5.92	5.29	5.55	5.26	6.13
HCC2998			18.8	4.71	6.33	4.31	5.36	4.77	5.10	4.43
HT29	4.85	2.63	15.7	4.05	7.77	6.49	4.69	5.18	5.52	7.76
CNS cancer										
SF-268	3.19	>25	>25	>25	ND ^c	16.6	>25	>25	2.86	>25
SF-539	>25	4.46	>25	5.17	4.50	10.5	10.8	5.01	19.5	14.6
U251	9.49	3.46	14.0	5.04	6.49	5.53		4.35	6.01	6.28
melanoma										
LOX IMVI	5.15	0.84	16.7	5.35	4.92	5.91	4.86	4.69	6.23	ND ^c
SK-MEL-5	4.57	4.37	>25	5.10	5.98	8.83	7.04	7.71	10.8	9.69
ovarian cancer										
OVCAR-3	13.3	4.00	>25	4.73	6.64	6.77	5.25	5.19	5.66	5.78
OVCAR-8	8.72	1.97	13.5	5.19	4.78	5.53	4.88	8.02	4.76	5.13
renal cancer										
786-0	7.54	1.44	18.5	4.30	11.5	8.69	8.45	7.18	9.23	8.44
SN12C	5.08	3.46	13.4	4.38	6.90	7.73	6.05	6.46	5.40	8.30
UO-31	0.39	2.95	>25	0.47	9.41	9.55	9.97	8.74	15.3	11.0
prostate cancer										
PC-3	9.73	4.22	16.0	5.51	7.36	6.34	7.15	6.88	7.77	7.21
breast cancer										
NCI/ADR-RES	>25	6.05	14.6	5.53	5.66	6.44	5.34	8.20	5.44	5.55
BT-549	>25	5.07	13.0	5.89	5.62	5.75	5.16	6.20	5.05	4.19
T-47D	8.35	4.09	16.9	4.92	8.39	8.22	6.69	9.27	8.41	7.30
MG-MID ^b	11.5	3.55	19.6	5.51	7.98	8.62	7.41	8.13	8.25	8.91

^a GI₅₀ represents the compound concentration (μM) required to achieve 50% inhibition of tumor cell growth. ^b MG MID represents the calculated mean GI₅₀ for all panels. ^c Not determined.

pattern, except that the NCI-H522 nonsmall cell lung cancer cell line is more sensitive to this compound (GI₅₀ = 0.89 μM). The less potent Cdc25A inhibitors, lactone **9** and its double-bond-saturated derivative **16**, also showed comparable growth inhibition effects among the eight different cancer types with MG-MID at 11.5 μM and 5.51 μM, respectively. This may be due to hydrolysis of the lactone into a hydroxyl carboxylic acid by cellular esterases. Compounds **9** and **16** differed from each other in that **9** potently inhibited the NCI-H522 nonsmall cell lung cancer cell line (GI₅₀ = 0.89 μM) and the SF-268 central nerve system cancer cell line (GI₅₀ = 3.19 μM), which were insensitive to compound **16**. This may be due to inhibition of some cellular enzymes, specifically expressed in these cell lines, by compound **9** with a mechanism related to the double bond conjugated to the cyano group. Compounds **16** and **9** also showed distinct selectivity in the UO-31 renal cancer cell lines (GI₅₀ = 0.39 and 0.47 μM, respectively).

Compound **13** showed very good growth inhibitory activity (GI₅₀ = 3.55 μM), although it is not active in the Cdc25A enzyme inhibition assay. It was also observed that the selectivity over different tumor cell lines of **13** was different from other compounds tested. It was more selective for the LOX IMVI melanoma cell line (GI₅₀ = 0.84 μM), the OVCAR-8 ovarian cancer cell line (GI₅₀ = 1.97 μM), the 786-0 (GI₅₀ = 1.44 μM) and UO-31 (GI₅₀ = 2.95 μM) renal cancer cell lines, and the HT29 colon cancer cell line (GI₅₀ = 2.63 μM). The antiproliferative effects of compound **13** might arise from inhibition of other cellular enzymes.

Compounds **10** and **9** were shown to block anchorage independent growth of tumor cells in soft agar clonogenic assays. At 10.9 and 12.0 μM, respectively, com-

pounds **9** and **10** reduced the HT-29 colon cancer cell colony number to 50% of the control. In addition, compound **9** reduced the colony number of A549 human lung adenocarcinoma cells by 50% at 7.2 μM.

Conclusion

Unusual chemical transformations of readily available natural products such as cholesteryl acetate were used to synthesize small molecule inhibitors for protein phosphatases, especially for Cdc25A dual-specificity protein phosphatase, an oncogenic protein that is overexpressed in several human tumor cell lines. Silica gel supported pyrolysis of an azido-homo-oxa steroid led to rearrangement, presumably by a mechanism similar to that of solution phase Schmidt fragmentation, to produce a group of novel and potent inhibitors of human Cdc25A phosphatase.

Cyano-containing acid **17**, one of the best inhibitors in this group, inhibited the activity of Cdc25A protein phosphatase, reversibly and noncompetitively, with an IC₅₀ value of 2.2 μM. These results suggest that compounds such as **17** may interact with Cdc25A, presumably with an arginine group at a site distinct from the substrate binding site. Compound **17** inhibited human Cdc25C phosphatase with an IC₅₀ of 6.5 μM. The inhibition of receptor protein tyrosine phosphatase CD45 by compound **17** (IC₅₀ = 8.3 μM) was most consistent with a mixed inhibition model.

Other simpler steroidal derived acids were synthesized, using conventional methods, to evaluate structure-activity relationships. It was observed that a phosphate surrogate such as a carboxyl or a xanthate group is required for inhibitory activity. A hydrophobic alkyl chain, such as the cholesteryl side chain, contributes

greatly to the potency.²² Acid **26** and xanthate **27** showed better selectivity over Cdc25A with an IC₅₀ of 5.1 μ M and 1.1 μ M, respectively, and their IC_{50s} toward receptor tyrosine phosphatase, CD45, were greater than 100 μ M.

The steroidal derived Cdc25A inhibitors described herein provide unique leads for the development of PTPase inhibitors, which previously employ the common approach of incorporation of nonhydrolyzable phosphate groups in synthetic peptide¹⁵ or peptidomimetic substrates.³¹ It is expected that compounds with structures significantly different from natural steroids might be better candidates for drug development since they are less likely to interfere with or be eliminated by hormonal pathways. It was observed that simple steroidal acids, such as compounds **14** and **27**,²² although exhibiting very potent Cdc25A inhibition, did not inhibit *in vitro* growth of tumor cells as well as other Cdc25A inhibitors with more complex structures. This may result from poor penetration through the plasma membrane or increased ease of elimination by the metabolic pathways.

Experimental Section

Starting materials were purchased from Aldrich. Thin-layer chromatography analysis (TLC) was performed on aluminum sheets precoated with 0.2 mm of silica gel containing 60F254 indicator. Spots were detected with shortwave UV light or Ceric sulfate spray. Flash chromatography was run using 230–400 mesh silica gel. Reverse phase high performance liquid chromatography (HPLC) was run on a Phenomenex LUNA 5 μ m C18 semipreparative column. The homogeneity of all the compounds was routinely checked by TLC on silica gel plates and also by HPLC. Melting points were measured on a Kofler hot stage apparatus attached to a digital thermometer and were uncorrected. Optical rotations were taken on a JASCO DIP-360 digital polarimeter. Fourier transformed infrared spectra were obtained on a Nicolet 520 FTIR spectrometer. ¹H (300 or 400 MHz) and ¹³C (75 or 100 MHz) NMR and DEPT spectra were recorded on either a Varian Gemini-300 or on a Varian XL-400 spectrometer. Chemical shifts are reported relative to CDCl₃ (δ 7.24). High resolution mass spectra (EI or FAB) were recorded on a VG Analytical 70-SE mass spectrometer equipped with a 11-250J data system. Elemental analyses were performed by Atlantic Microlab, Norcross, GA.

The syntheses of compounds **1**,²⁰ **7**,²⁰ **14**,²⁰ **27**,²⁷ **34**,²⁸ **35**,²⁹ and **37**³⁰ were performed as previously reported except as indicated.

3- β -Acetoxy-5,6-seco-5-oxo-cholestan-6-oic acid (1). Ozone was passed into a stirred and cooled (chloroform/dry ice bath) solution of cholesteryl acetate (12 g, 28 mmol) in 300 mL of petroleum ether for 30 min until the solution turned light blue. Piperidine (5 mL, 50 mmol) was then added dropwise over 3 min. The volume of solution was reduced to 100 mL after being stirred and warmed in room temperature for 3 h. The white precipitates were separated and washed with 2 M HCl (3 \times 25 mL) and with water (1 \times 30 mL) to obtain the free acid. Flash chromatography of the crude acid over silica gel, using hexanes–EtOAc (3:1), afforded compound **1** (5.5 g, 41%) as colorless crystals: mp 115–117 $^{\circ}$ C (lit.²⁰ 115–116 $^{\circ}$ C); FTIR (neat film) 3400–2500 (br), 2960, 2868, 1736, 1716, 1249 cm⁻¹; ¹H NMR (CDCl₃, 300 MHz) δ 9.89 (broad), 5.29 (brs, 1 H), 3.11 (dd, J = 14.4, 4.3 Hz, 1 H), 2.33 (d, J = 14.5 Hz, 1 H), 2.08 (s, 3 H), 0.99 (s, 3 H), 0.88 (d, J = 6.4 Hz, 3 H), 0.83 (d, J = 6.6 Hz, 6 H), 0.65 (s, 3 H); ¹³C NMR and DEPT (CDCl₃, 100 Hz) δ 216.4 (C), 178.6 (C), 170.3 (C), 73.5 (CH), 55.9 (CH), 54.4 (CH), 52.3 (C), 43.1 (CH₂), 42.5 (C), 41.5 (CH), 39.7 (CH₂), 39.4 (CH₂), 35.9 (CH₂), 35.7 (CH), 35.5 (CH), 34.4 (CH₂), 34.1 (CH₂), 27.9 (CH), 27.9 (CH₂), 25.1 (CH₂), 24.3 (CH₂), 23.7 (CH₂), 23.0 (CH₂), 22.8 (CH₃), 22.5 (CH₃), 21.5 (CH₃), 18.5 (CH₃), 17.6

(CH₃), 11.6 (CH₃); CIMS m/z (relative intensity) 477 (M⁺ + 1, 4), 417 (M⁺ – AcOH + 1, 88), 399 (100), 357 (40), 331 (45).

3- β -Acetoxy-B-homo-6-oxa-4-cholesten-7-one (2).²⁶ SOCl₂ (0.8 mL, 10 mmol) in 2 mL of CH₂Cl₂ was added dropwise to a stirred and cooled (0 $^{\circ}$ C) solution of 3- β -acetoxy-5,6-seco-5-oxo-cholestan-6-oic acid (**1**) (2.3 g, 5 mmol) in 12 mL of CH₂Cl₂. After the mixture was stirred at 0 $^{\circ}$ C for 30 min, 0.1 mL of pyridine was added, and the resulting mixture was stirred at room temperature for 2 h. Then the solvent was evaporated *in vacuo* to yield a residue which was chromatographed on silica gel to yield 3- β -acetoxy-B-homo-6-oxa-4-cholesten-7-one (**2**) (1.92 g, 78%) as a colorless oil: UV λ_{\max} (CHCl₃) 241.6 nm (ϵ = 358); FTIR (neat film) 2939, 2873, 1766, 1740, 1667, 1648, 1375, 1242, 1123 cm⁻¹; ¹H NMR (CDCl₃, 300 MHz) δ 5.50 (d, J = 4.2 Hz, 1 H), 5.33 (t, J = 3.3 Hz, 1 H), 2.37 (m, 2 H), 2.04 (s, 3 H), 1.03 (s, 3 H), 0.88 (d, J = 6.6 Hz, 3 H), 0.85 (d, J = 6.6 Hz, 6 H) 0.68 (s, 3 H); EIMS m/z (relative intensity) 458 (22), 498 (35), 370 (100), 110(62); EI HRMS calcd for C₂₉H₄₆O₄ m/z 458.3396, found 458.3408.

3- α -Azido-B-homo-6-oxa-4, 5-cholesten-7-one (3). To a stirred solution of 2.40 g (5 mmol) of crude 3- β -acetoxy-B-homo-6-oxa-4-cholesten-7-one (**2**) in 35 mL of acetone was added dropwise a solution of NaN₃ (650 mg, 10 mmol) in 5 mL of water. The reaction mixture was stirred at room temperature for 2 h, poured into 50 mL water, and extracted with ether. The ethereal extracts were dried over MgSO₄ and concentrated *in vacuo* to yield a residue which was subjected to silica gel column chromatography (230–400 mesh, hexane/EtOAc = 10:1) to afford compound **3**, 1.17 g (55.3%) as a yellowish oil: [α]_D²⁰ +98.3 $^{\circ}$ (c 0.6, CHCl₃); UV λ_{\max} (CHCl₃) 245 nm (ϵ = 899); FTIR (neat film): 2949, 2873, 2094, 1763, 1670, 1247 cm⁻¹; ¹H NMR (CDCl₃, 300 MHz) δ 5.43 (d, J = 2.5 Hz, 1 H), 4.07 (m, 1 H), 2.44 (d, J = 15.0, 11.0 Hz, 1 H), 2.38 (dd, J = 15.0, 2.0 Hz, 1 H), 0.99 (s, 3 H), 0.89 (d, J = 6.5 Hz, 3 H), 0.84 (d, J = 6.6 Hz, 6 H), 0.65 (s, 3 H); ¹³C NMR and DEPT (CDCl₃, 100 Hz) δ 172.1 (C), 160.0 (C), 113.5 (CH), 57.4 (CH), 56.3 (CH), 55.4 (CH), 51.7 (CH), 42.9 (C), 39.5 (CH₂), 39.4 (CH₂), 39.0 (C), 37.0 (CH₂), 35.9 (CH₂), 35.6 (CH), 34.9 (CH), 33.9 (CH₂), 28.0 (CH), 27.6 (CH₂), 25.0 (CH₂), 23.8 (CH₂), 23.7 (CH₂), 22.8 (CH₃), 22.6 (CH₃), 22.5 (CH₂), 19.2 (CH₃), 18.5 (CH₃), 11.8 (CH₃); CIMS m/z (relative intensity) 442 (M⁺ + 1, 17), 414 (M⁺ – N₂ + 1, 100), 399 (M⁺ – N₃, 26). Anal. (C₂₇H₄₄N₃O₂·0.25 hexane) C, H, N.

General Method of Syntheses and Purification of Compounds 4–13. A solution of **3** (4.4 g, 10 mmol) in 15 mL of EtOAc was poured onto 16 g of silica gel (0.040–0.063 mm, EM Science Co.). The solvent was allowed to evaporate in the hood. Then, the 3- α -azido-B-homo-6-oxa-4,5-cholesten-7-one (**3**) coated silica gel was pyrolyzed at 180 $^{\circ}$ C for 1 h and then extracted with EtOAc (3 \times 200 mL) and methanol (2 \times 200 mL). The resulting solutions were combined and concentrated, *in vacuo*, to yield a residue that was subjected to column chromatography (silica gel 230–400 mesh, hexane/EtOAc = 20:1~3:1) to afford (10S)-1,4,6-trioxo-2-cholesten (**4**) (12 mg, 0.29%), 6-oxa-2,4-cholest-dien-7-one (**5**) (60 mg, 1.5%), and briefly separated eluents of compounds **6–13**. Further flash chromatography of these eluents on silica gel (hexane/EtOAc = 2:1) afford 5,6-seco-5-oxo-2-cholesten-6-oic acid (**6**) (78 mg, 1.9%), 5,6-seco-5-oxo-3-cholesten-6-oic acid (**7**) (1.70 g, 41.9%), cyano-containing lactones **8** (53 mg, 1.3%) and **9** (392 mg, 9.5%), A-Homo-6-aza-3-cholesten-5,6a-dione (**13**) (24 mg, 0.58%), and mixtures of cyano-containing acid isomers **10–12** (841 mg, 20.4%). Even though the TLC R_f values of compounds **6–13** were about the same using hexane/EtOAc = 2:1 on silica gel plates, these compounds were eluted from a silica gel column in the order of **6**, **10–12**, **7**, **8**, **9**, and **13**. Pure isomers were obtained by reverse phase HPLC (Phenomenex LUNA 5 μ m C18) using 100% acetonitrile. From peak areas in the HPLC chromatogram and known total weight, the following yields were calculated: **10** (400 mg, 9.7%), **11** (215 mg, 5.2%), **12** (226 mg, 5.5%).

(10S)-2-cholesten-1,4,6-trione (4) was obtained as light yellow crystals: mp 162–164 $^{\circ}$ C; FTIR (neat film) 2924, 2862, 1712, 1687, 1457, 1377, 1265, 1072, 848 cm⁻¹; ¹H NMR (CDCl₃,

300 Hz) δ 6.69 (dd, $J = 10.2, 1.5$ Hz, 1 H), 6.50 (d, $J = 10.2$ Hz, 1 H), 3.39 (s, 1 H), 2.42 (m, 2 H), 2.11 (dt, $J = 13.0, 3.0$ Hz, 1 H), 1.97–1.81 (m, 3 H), 1.70 (m, 1 H), 1.43 (s, 3 H), 0.93 (d, $J = 6.5$ Hz, 3H), 0.87 (d, $J = 6.6$ Hz, 6 H), 0.82 (s, 3 H); ^{13}C NMR (CDCl₃, 100 MHz) δ 206.0 (C), 201.0 (C), 196.4 (C), 140.1 (CH), 139.1 (CH), 71.6 (CH), 57.0 (CH), 55.8 (CH), 55.3 (C), 51.0 (CH), 47.2 (CH₂), 42.9 (C), 39.7 (CH₂), 39.4 (CH₂), 37.7 (CH), 36.1 (CH₂), 35.7 (CH), 28.0 (CH₂), 28.0 (CH), 26.1 (CH₃), 24.0 (CH₂), 23.8 (CH₂), 22.8 (CH₃), 22.5 (CH₃), 21.5 (CH₂), 18.7 (CH₃), 11.7 (CH₃); EI MS m/z (relative intensity) 412 (M⁺, 78), 397 (M⁺ – CH₃, 20), 288 (25), 124 (100). Anal. (C₂₇H₄₀O₃) C, H.

6-Oxa-2,3,4,5-cholest-dien-7-one (5) was obtained as colorless oil: FTIR (neat film) 2947, 2847, 1768, 1657 cm⁻¹; ^1H NMR (CDCl₃, 300 MHz) δ 5.91 (ddd, $J = 5.7, 3.6, 3.5$ Hz, 1 H), 5.69 (d, $J = 5.5$ Hz, 1 H), 5.67 (ddd, $J = 5.7, 5.4, 2.5$ Hz, 1 H), 2.50 (d, $J = 12.3$ Hz, 1H), 2.37 (d, $J = 12.4$ Hz, 1 H), 2.47 (d, $J = 18.3$ Hz, 1 H), 2.27 (d, $J = 17.5, 2.8$ Hz, 1 H), 1.02 (s, 3 H), 0.89 (d, $J = 6.5$ Hz, 3 H), 0.86 (d, $J = 6.5$ Hz, 6 H), 0.68 (s, 3 H); ^{13}C NMR and DEPT (CDCl₃, 100 Hz) δ 173.4 (C), 157.6 (C), 123.5 (CH), 123.2 (CH), 111.6 (CH), 56.4 (CH), 55.4 (CH), 45.9 (CH), 43.1 (C), 39.4 (CH₂), 39.4 (CH₂), 37.8 (C), 37.2 (CH₂), 36.3 (CH₂), 35.1 (CH), 35.1 (CH), 28.0 (CH), 27.7 (CH₂), 25.0 (CH₂), 23.8 (CH₂), 22.8 (CH₂), 22.5 (CH₃), 18.6 (CH₃), 18.0 (CH₂), 11.9 (CH₃); EIMS m/z (relative intensity) 398 (M⁺, 20), 370 (10), 329 (22), 247 (23), 149 (40), 109 (100); EI HRMS calcd for C₂₇H₄₂O₂ m/z 398.3185, found 398.3187.

5,6-Seco-5-oxo-2,3-cholesten-6-oic acid (6) was obtained as colorless oil: FTIR (neat film) 3400–2500 (br), 2951, 2867, 1738, 1706, 1466, 1380, 1240, 1045, 926, 676 cm⁻¹; ^1H NMR (CDCl₃, 300 Hz) δ 5.68 (m, 2 H), 3.21 (d, $J = 21.1$ Hz, 1 H), 2.85 (d, $J = 22.5$ Hz, 1 H), 2.46 (dd, $J = 17.4, 5.5$ Hz, 1 H), 2.27 (dd, $J = 16.6, 2.7$ Hz, 1 H), 2.09 (dd, $J = 16.6, 7.5$ Hz, 1 H), 2.00 (m, 3 H), 1.99 (m, 1 H), 1.98 (m, 1 H), 1.88 (m, 3 H), 1.83–1.20 (m, 10 H), 1.05 (s, 3 H), 0.86 (d, $J = 6.6$ Hz, 3 H), 0.82 (d, $J = 6.6$ Hz, 6 H), 0.65 (s, 3 H); ^{13}C NMR (CDCl₃, 100 MHz) δ 217.1 (C), 178.9 (C), 126.0 (CH), 124.4 (CH), 55.8 (CH), 55.6 (CH), 50.9 (C), 42.6 (C), 40.9 (CH), 40.4 (CH₂), 39.8 (CH₂), 39.4 (CH₂), 39.1 (CH₂), 36.0 (CH₂), 35.7 (CH), 35.6 (CH), 35.4 (CH₂), 28.0 (CH₂), 28.0 (CH), 24.2 (CH₂), 24.0 (CH₂), 23.8 (CH₂), 22.8 (CH₃), 22.5 (CH₃), 18.6 (CH₃), 16.8 (CH₃), 11.7 (CH₃); FAB MS m/z (relative intensity) 417 (M⁺ + 1, 48), 399 (M⁺ + 1 – H₂O, 100), 381 (30), 247 (50); FAB HRMS calcd for C₂₇H₄₃NO₂ m/z 417.3369 (M⁺ + 1), found 417.3337.

5,6-Seco-5-oxo-3,4-cholesten-6-oic acid (7) was obtained as colorless oil: FTIR (neat film) 3400–2500 (br), 2916, 1747, 1712, 1677, 1466, 1389, 1228 cm⁻¹; ^1H NMR (CDCl₃, 300 MHz) δ 6.73 (m, 1 H), 5.88 (dd, $J = 10.5, 1.5$ Hz, 1 H), 2.40 (dd, $J = 15.5, 5.0$ Hz, 1 H), 1.10 (s, 3 H), 0.90 (d, $J = 6.5$ Hz, 3 H), 0.86 (d, $J = 6.6$ Hz, 6 H), 0.69 (s, 3 H); EIMS m/z (relative intensity) 416 (M⁺, 17), 398 (23), 354 (32), 333 (55), 247 (63), 110 (100); EI HRMS calcd for C₂₇H₄₄O₃ m/z 416.3290, found 416.3272.

Compound 8 was obtained as colorless prisms: mp 132–134 °C; $[\alpha]_D^{20} + 39.3^\circ$ (c 0.52, CHCl₃); UV λ_{max} (CHCl₃) 242.6 nm ($\epsilon = 152$); FTIR (neat film) 2954, 2870, 2224, 1733, 1473, 1389, 1256 cm⁻¹; ^1H NMR (CDCl₃, 300 MHz) δ 6.54 (dt, $J = 11.0, 7.8$ Hz, 1 H), 5.35 (d, $J = 11.1$ Hz, 1 H), 2.63 (m, 2 H), 2.61 (dd, $J = 18.0, 5.1$ Hz, 1 H), 2.08 (dt, $J = 12.1, 3.0$ Hz, 1 H), 2.02 (dd, $J = 18.0, 11.5$ Hz, 1 H), 2.01–1.68 (m, 5 H), 1.43 (s, 3 H), 0.91 (d, $J = 6.6$ Hz, 3 H), 0.86 (d, $J = 6.3$ Hz, 6 H), 0.70 (s, 3 H); ^{13}C NMR and DEPT (CDCl₃, 100 Hz) δ 170.6 (C), 154.4 (CH), 115.8 (C), 100.2 (CH), 86.3 (C), 55.9 (CH), 55.8 (CH), 49.3 (CH), 42.6 (C), 39.4 (CH₂), 39.1 (CH₂), 36.0 (CH₂), 35.7 (CH₂), 35.6 (CH), 34.8 (CH₂), 30.9 (CH), 28.1 (CH₂), 28.0 (CH), 26.1 (CH₂), 26.0 (CH₃), 23.8 (CH₂), 23.4 (CH₂), 22.9 (CH₂), 22.8 (CH₃), 22.5 (CH₃), 18.7 (CH₃), 12.0 (CH₃); EIMS m/z (relative intensity) 413 (M⁺, 45), 398 (24), 385 (27), 333 (31), 248 (33), 135 (100); EI HRMS calcd for C₂₇H₄₃NO₂ m/z 413.3294, found 413.3308. Anal. (C₂₇H₄₃NO₂) C, H, N.

Compound 9 was obtained as colorless prisms: mp 109–111 °C; $[\alpha]_D^{20} - 42.1^\circ$ (c 0.73, CHCl₃); UV λ_{max} (CHCl₃) 240.8 nm ($\epsilon = 89.7$); FTIR (neat film) 3071, 2956, 2871, 2219, 1720, 1390, 1259 cm⁻¹; ^1H NMR (CDCl₃, 300 MHz) δ 6.52 (dt, $J = 10.8, 7.8$ Hz, 1 H), 5.32 (d, $J = 10.5$ Hz, 1 H), 2.60 (dd, $J = 17.7, 4.8$

Hz, 1 H), 2.55 (m, 2 H), 2.07 (dt, $J = 12.0, 2.7$ Hz, 1 H), 2.00 (dd, $J = 17.7, 11.5$ Hz, 1 H), 1.99–1.77 (m, 5 H), 1.34 (s, 3 H), 0.90 (d, $J = 6.0$ Hz, 3 H), 0.86 (d, $J = 6.6$ Hz, 6 H), 0.70 (s, 3 H); ^{13}C NMR and DEPT (CDCl₃, 100 Hz) δ 170.8 (C), 154.5 (CH), 115.9 (C), 99.8 (CH), 86.6 (C), 55.7 (CH), 55.6 (CH), 44.5 (CH), 42.5 (C), 39.4 (CH₂), 38.9 (CH₂), 38.2 (CH₂), 36.0 (CH₂), 35.7 (CH₂), 35.6 (CH), 30.8 (CH), 28.0 (CH₂), 28.0 (CH), 25.8 (CH₂), 23.7 (CH₂), 23.5 (CH₂), 23.0 (CH₃), 22.8 (CH₃), 22.8 (CH₂), 22.5 (CH₃), 18.6 (CH₃), 11.9 (CH₃); EIMS m/z (relative intensity) 413 (M⁺, 5), 398 (2), 385 (2), 353 (5), 333 (46), 290 (21), 248 (28), 135 (100); CIMS m/z (relative intensity) 414 (M⁺ + 1, 100), 396 (37), 333 (18), 135 (22); EI HRMS calcd for C₂₇H₄₃NO₂ m/z 413.3294, found 413.3253. Anal. (C₂₇H₄₃NO₂) C, H, N.

Compound 10 was obtained as a colorless oil: $[\alpha]_D^{20} + 31.0^\circ$ (c 0.35, CHCl₃); UV λ_{max} (CHCl₃) 255.6 nm ($\epsilon = 814$); HPLC (acetonitrile, 4 mL/min, 205 nm) 11.04 min; FTIR (neat film) 3380–2500 (br), 3728, 2953, 2874, 2229, 1703, 1459, 1288 cm⁻¹; ^1H NMR (CDCl₃, 300 MHz) δ 6.50 (dt, $J = 11.0, 7.2$ Hz, 1 H), 5.33 (d, $J = 11.0$ Hz, 1 H), 4.93 (s, 1 H), 4.84 (s, 1 H), 2.59 (m, 2 H), 2.35 (dd, $J = 15.0, 3.3$ Hz, 1 H), 2.10 (dd, $J = 15.0, 6.6$ Hz, 1 H), 2.17 (t, $J = 7.2$ Hz, 2 H), 1.97 (m, 3 H), 0.90 (d, $J = 6.6$ Hz, 3H), 0.86 (d, $J = 6.6$ Hz, 6 H), 0.68 (s, 3 H); ^{13}C NMR and DEPT (CDCl₃, 100 Hz) δ 179.1 (C), 154.7 (CH), 150.2 (C), 116.0 (C), 111.2 (CH₂), 99.8 (CH), 56.0 (CH), 55.3 (CH), 51.4 (CH), 43.0 (C), 39.6 (CH₂), 39.5 (CH₂), 37.2 (CH₂), 36.1 (CH₂), 35.8 (CH), 35.7 (CH), 32.5 (CH₂), 29.9 (CH₂), 29.0 (CH₂), 28.0 (CH), 28.0 (CH₂), 24.4 (CH₂), 23.8 (CH₂), 22.8 (CH₃), 22.5 (CH₃), 18.7 (CH₃), 11.9 (CH₃); EIMS m/z (relative intensity) 413 (M⁺, 34), 395 (100), 380 (25), 354 (67), 333 (23), 282 (44), 240 (40), 43 (98); EI HRMS calcd for C₂₇H₄₃NO₂ m/z 413.3294, found 413.3279. Anal. (C₂₇H₄₃NO₂) C, H, N.

Compound 11 was obtained as a colorless oil: $[\alpha]_D^{20} + 12.7^\circ$ (c 0.15, CHCl₃); UV λ_{max} (CHCl₃) 255.0 nm ($\epsilon = 1067$); HPLC (acetonitrile, 4 mL/min, 205 nm) 10.56 min; FTIR (neat film) 3400–2500 (br), 2955, 2874, 2224, 1711, 1649, 1470, 1386, 1292 cm⁻¹; ^1H NMR (CDCl₃, 300 MHz) δ 6.37 (dt, $J = 10.9, 7.7$ Hz, 1 H), 5.27 (d, $J = 10.9, 1.1$ Hz), 5.18 (t, $J = 7.7$ Hz, 1 H), 3.10 (dt, $J = 7.7, 5.5$ Hz, 2 H), 2.22 (dd, $J = 15.4, 3.3$ Hz, 1H), 2.04 (dd, $J = 15.4, 7.6$ Hz, 1H), 1.98 (m, 3H), 1.67 (s, 3 H), 0.90 (d, $J = 6.6$ Hz, 3 H), 0.86 (d, $J = 6.6$ Hz, 6 H), 0.68 (s, 3 H); EIMS m/z (relative intensity) 413 (M⁺, 15), 395 (28), 354 (25), 333 (12), 240 (17), 43 (100); EI HRMS calcd for C₂₇H₄₃NO₂ m/z 413.3294, found 413.3312. Anal. (C₂₇H₄₃NO₂) C, H, N.

Compound 12 was obtained as a colorless oil: $[\alpha]_D^{20} + 26.6^\circ$ (c 0.30, CHCl₃); UV λ_{max} (CHCl₃) 255.4 nm ($\epsilon = 1212.4$); HPLC (acetonitrile, 4 mL/min, 205 nm) 12.11 min; FTIR (neat film) 3400–2500 (br), 2946, 2871, 2221, 1704, 1704, 1647, 1470, 1388, 1294 cm⁻¹; ^1H NMR (CDCl₃, 300 MHz) δ 6.38 (dt, $J = 11.1, 7.5$ Hz, 1 H), 5.27 (d, $J = 10.4$ Hz, 1 H), 5.17 (t, $J = 7.2$ Hz, 1 H), 3.08 (t, $J = 7.2$ Hz, 2 H), 2.22 (dd, $J = 15.4, 4.4$ Hz, 1H), 2.07 (dd, $J = 15.4, 6.6$ Hz, 1H), 1.94 (m, 3H), 1.60 (s, 3 H), 0.90 (d, $J = 6.6$ Hz, 3 H), 0.86 (d, $J = 6.6$ Hz, 6 H), 0.68 (s, 3 H); EIMS m/z (relative intensity) 413 (M⁺, 20), 395 (57), 354 (50), 333 (12), 282 (32), 240 (32), 43 (100); EI HRMS calcd for C₂₇H₄₃NO₂ m/z 413.3294, found 413.3271. Anal. (C₂₇H₄₃NO₂) C, H, N.

A-Homo-6-aza-3-cholesten-5,6a-dione (13) was obtained as white crystals: mp 187–188 °C; FTIR (neat film) 2949, 2864, 1721, 1645, 1391, 1221, 1179 cm⁻¹; ^1H NMR (CDCl₃, 300 Hz) δ 6.74 (ddd, $J = 10.4, 7.7, 2.7$ Hz, 1 H), 6.21 (dd, $J = 10.4, 2.7$ Hz, 1 H), 2.43 (dd, $J = 17.6, 4.4$ Hz, 1 H), 2.41–2.22 (m, 2 H), 2.16 (dd, $J = 14.8, 6.6$ Hz, 1 H), 2.07 (dt, $J = 13.2, 3.3$ Hz, 1 H), 1.92 (dd, $J = 17.6, 12.5$ Hz, 1 H), 1.30 (s, 3 H), 0.90 (d, $J = 6.6$ Hz, 3 H), 0.86 (d, $J = 6.6$ Hz, 6 H), 0.71 (s, 3 H); ^{13}C NMR (CDCl₃, 100 MHz) δ 175.7, 169.3, 149.6, 128.8, 62.0, 56.2, 55.9, 42.8, 42.3, 39.4, 39.1, 39.1, 37.5, 36.0, 35.6, 30.2, 28.1, 28.0, 25.2, 23.7, 23.7, 23.1, 22.8, 22.5, 22.3, 18.7, 11.9; EI MS m/z (relative intensity) 413 (M⁺, 30), 385 (20), 332 (100), 124 (60). Anal. (C₂₇H₄₃NO₂) C, H, N.

Hydrogenation of Compounds 5, 7, and 9–13. General procedure of the hydrogenation: To a solution of a compound in ethyl acetate was added 10% Pd/C. The resulting mixture

was stirred and hydrogenated at atmospheric pressure until 1 equiv of hydrogen was absorbed, and then the reaction solution was filtered through Celite. The filtrate was concentrated in vacuo to yield the product.

B-Homo-5-oxa-4-cholesten-7-one (14) was obtained through hydrogenation of **5** as a colorless oil: FTIR (neat film) 2933, 2874, 1756, 1457, 1130 cm^{-1} ; $^1\text{H NMR}$ (CDCl_3 , 300 MHz) δ 5.38 (t, $J = 3.2$ Hz, 1 H), 2.40 (m, 2 H), 1.89 (m, 2 H), 0.97 (s, 3 H), 0.87 (d, $J = 6.6$ Hz, 3 H), 0.84 (d, $J = 6.6$ Hz, 6 H), 0.67 (s, 3 H); $^{13}\text{C NMR}$ (CDCl_3 , 100 MHz) 173.8 (C), 155.6 (C), 114.3 (CH), 56.4 (CH), 55.6 (CH), 51.3 (CH), 43.0 (C), 39.7 (CH_2), 39.4 (CH_2), 38.5 (C), 37.2 (CH_2) 35.9 (CH_2), 35.7 (CH), 34.9 (CH_2), 34.8 (CH), 28.0 (CH), 27.7 (CH_2), 25.1 (CH_2), 24.2 (CH_2), 23.8 (CH_2), 22.8 (CH_3), 22.5 (CH_3), 22.1 (CH_2), 19.1 (CH_3), 18.6 (CH_3), 17.1 (CH_2), 11.9 (CH_3); EI MS m/z (relative intensity) 400 (M^+ , 15), 372 (100), 330 (73), 111 (50); EI HRMS calcd for $\text{C}_{27}\text{H}_{44}\text{O}_2$ m/z 400.3341, found 400.3361.

5,6-Seco-5-oxo-cholestan-6-oiic acid (15)²⁰ was obtained through hydrogenation of compound **7** as colorless oil: $^1\text{H NMR}$ (CDCl_3 , 300 MHz) δ 3.18 (m, 1 H), 2.26–1.99 (m, 6 H), 0.98 (s, 3 H), 0.88 (d, $J = 0.66$ Hz, 3 H), 0.84 (d, $J = 0.66$ Hz, 6 H), 0.66 (s, 3 H).

Compound 16 was obtained through hydrogenation of compound **9** as colorless oil: $[\alpha]_D^{20} -9.2^\circ$ (c 0.5, CHCl_3); FTIR (neat film) 2952, 2873, 2250, 1726, 1468, 1388, 1256, 977 cm^{-1} ; $^1\text{H NMR}$ (CDCl_3 , 300 MHz) δ 2.60 (dd, $J = 17.7$, 4.8 Hz, 1 H), 2.36 (t, $J = 6.6$ Hz, 2 H), 2.06 (m, 1 H), 1.97 (dd, $J = 17.7$, 11.4 Hz, 1 H), 0.90 (d, $J = 6.6$ Hz, 3 H), 0.86 (d, $J = 6.6$ Hz, 6 H), 0.70 (s, 3 H); EIMS m/z (relative intensity): 415 (M^+ , 12), 400 (22), 355 (15), 333 (38), 248 (30), 135 (100); CI HRMS m/z calcd for $\text{C}_{27}\text{H}_{46}\text{NO}_2$ m/z 416.3529 (M^+ + 1), found 416.3520.

Compound 17, 18, and 19. To a solution of a mixture of compounds **10, 11, and 12** (2:1:1, 100 mg, 0.24 mmol) in 15 mL of ethyl acetate was added 10 mg of 10% Pd/C. The resulting mixture was stirred and hydrogenated at atmospheric pressure for 30 min until 1 equiv of hydrogen was absorbed, and then the reaction solution was filtered through Celite. The filtrate was concentrated in vacuo and purified by reverse phase HPLC to afford **17** as a colorless oil: $[\alpha]_D^{20} +38.9^\circ$ (c 0.15, CHCl_3); HPLC (acetonitrile, 4 mL/min, 205 nm) $t_R = 11.09$ min; $^1\text{H NMR}$ (CDCl_3 , 300 MHz) δ 4.85 (s, 1 H), 4.78 (s, 1 H), 2.35 (m, 4 H), 0.95 (d, $J = 6.6$ Hz, 3 H), 0.85 (d, $J = 6.6$ Hz, 6 H), 0.75 (s, 3 H); $^{13}\text{C NMR}$ (CDCl_3 , 100 MHz) δ 179.1, 151.3, 119.7, 110.5, 56.0, 55.4, 51.4, 43.1, 39.7, 39.5, 37.3, 36.1, 35.9, 35.7, 29.3, 28.0, 28.0, 27.9, 26.9, 25.2, 24.4, 23.8, 22.8, 22.5, 18.7, 17.1, 12.0; EIMS m/z (relative intensity): 415 (M^+ , 15), 397 (53), 369 (28), 355 (50), 305 (100), 242 (80), 135 (93); EI HRMS calcd for $\text{C}_{27}\text{H}_{45}\text{NO}_2$ m/z 415.3450, found 415.3451. Compound **18** was obtained as colorless oil: HPLC (acetonitrile, 4 mL/min, 205 nm) $t_R = 10.65$ min; $^1\text{H NMR}$ (CDCl_3 , 300 MHz) δ 5.11 (t, $J = 6.9$ Hz, 1 H), 2.30 (t, $J = 7.2$ Hz, 2 H), 2.21–1.93 (m, 6 H), 1.65 (s, 3 H), 0.88 (d, $J = 6.6$ Hz, 3 H), 0.84 (d, $J = 6.6$ Hz, 6 H), 0.72 (s, 3 H); $^{13}\text{C NMR}$ (CDCl_3 , 100 MHz) δ 178.2, 139.8, 125.1, 119.7, 56.0, 55.2, 44.4, 43.1, 39.5, 39.5, 37.0, 36.1, 35.7, 34.9, 28.0, 27.9, 26.8, 26.2, 25.6, 24.4, 23.8, 22.8, 22.5, 19.2, 18.7, 16.6, 11.9; FAB MS m/z (relative intensity) 416 (M^+ + 1, 100), 398 (M^+ + 1 – H_2O , 60), 369 (28), 356 (45), 305 (18), 242 (25); FAB HRMS calcd for $\text{C}_{27}\text{H}_{46}\text{NO}_2$ m/z 416.3529 (M^+ + 1), found 416.3546.

Compound **19** was obtained as colorless oil: HPLC (acetonitrile, 4 mL/min, 205 nm) $t_R = 12.01$ min; $^1\text{H NMR}$ (CDCl_3 , 300 MHz) δ 5.13 (t, $J = 6.9$ Hz, 1 H), 2.30 (t, $J = 7.2$ Hz, 2 H), 2.26–2.02 (m, 4 H), 1.94 (m, 2 H), 1.55 (s, 3 H), 0.88 (d, $J = 6.6$ Hz, 3 H), 0.84 (d, $J = 6.6$ Hz, 6 H), 0.72 (s, 3 H); $^{13}\text{C NMR}$ (CDCl_3 , 100 MHz) δ 178.5, 140.0, 124.2, 119.9, 56.1, 55.0, 54.0, 43.1, 39.5, 39.5, 37.3, 36.0, 35.7, 35.2, 28.0, 28.8, 27.8, 26.5, 25.3, 24.6, 23.8, 22.8, 22.5, 18.7, 16.5, 12.9, 11.9; FAB MS m/z (relative intensity) 416 (M^+ + 1, 90), 398 (M^+ + 1 – H_2O , 100), 56 (60), 305 (40), 242 (45); FAB HRMS calcd for $\text{C}_{27}\text{H}_{46}\text{NO}_2$ m/z 416.3529 (M^+ + 1), found 416.3537.

Compound 20 was obtained through hydrogenation of **13** in methanol as a white solid: FTIR (neat film) 2947, 2868, 1742, 1673, 1459, 1400, 1176, 1163, 1150, 735 cm^{-1} ; $^1\text{H NMR}$ (CDCl_3 , 300 MHz) δ 2.71 (m, 2 H), 2.53 (ddd, $J = 8.1$, 5.2, 4.1

Hz, 2 H), 2.45 (dd, $J = 17.4$, 5.1 Hz, 1 H), 2.04 (m, 2 H), 1.94 (dd, $J = 17.4$, 11.1, 1 H), 1.29 (s, 3 H), 0.89 (d, $J = 6.6$ Hz, 3 H), 0.84 (d, $J = 6.6$ Hz, 6 H), 0.68 (s, 3 H); FABMS m/z (relative intensity): 416 (M^+ + 1, 100), 400 (30), 386 (5), 372 (10), 332 (10); FAB HRMS calcd for $\text{C}_{27}\text{H}_{46}\text{NO}_2$ m/z 416.3529 (M^+ + 1), found 416.3515.

Compounds 21 and 22. To a solution of compound **10** (25 mg, 0.061 mmol) in 2 mL of ethyl acetate was added 5 mg of 5% Pt/C. The resulting mixture was stirred and hydrogenated for 72 h and then filtered through Celite. The filtrate was concentrated in vacuo and separated by reverse phase HPLC using 100% acetonitrile to afford 10 mg of compound **21** as a colorless oil: HPLC (acetonitrile, 4 mL/min, 205 nm) $t_R = 14.21$ min; $^1\text{H NMR}$ (CDCl_3 , 300 MHz) δ 2.32 (t, $J = 6.9$ Hz, 2 H), 2.24 (d, $J = 4.8$ Hz, 2 H), 1.94 (m, 1 H), 0.89 (d, $J = 6.6$ Hz, 3 H), 0.88 (d, $J = 6.6$ Hz, 3 H), 0.84 (d, $J = 6.6$ Hz, 6 H), 0.67 (s, 3 H); $^{13}\text{C NMR}$ (CDCl_3 , 100 MHz) δ 178.6, 120.1, 56.2, 55.3, 48.9, 43.0, 39.6, 39.5, 37.1, 36.1, 35.8, 35.5, 29.5, 28.0, 27.9, 27.4, 25.7, 24.8, 23.8, 22.8, 22.5, 21.0, 19.0, 18.7, 17.1, 11.9; FABMS m/z (relative intensity): 418 (M^+ + 1, 32), 400 (100), 382 (55), 356 (35); FAB HRMS calcd for $\text{C}_{27}\text{H}_{48}\text{NO}_2$ m/z 418.3771 (M^+ + 1), found 418.3683. Compound **22** (8 mg) as colorless oil: HPLC (acetonitrile, 4 mL/min, 205 nm) $t_R = 12.96$ min; $^1\text{H NMR}$ (CDCl_3 , 300 MHz) δ 2.31 (m, 4 H), 1.94 (m, 1 H), 0.88 (d, $J = 6.6$ Hz, 3 H), 0.84 (d, $J = 6.6$ Hz, 6 H), 0.78 (d, $J = 7.2$ Hz, 3 H), 0.66 (s, 3 H); $^{13}\text{C NMR}$ (CDCl_3 , 100 MHz) δ 179.1, 119.8, 56.1, 54.8, 44.8, 43.0, 39.5, 39.5, 39.4, 36.1, 35.7, 35.5, 34.9, 31.9, 28.0, 27.9, 26.8, 25.5, 24.8, 23.8, 22.8, 22.5, 20.2, 18.7, 17.1, 13.6, 11.7; FABMS m/z (relative intensity): 418 (M^+ + 1, 25), 400 (100), 382 (45), 356 (20); FAB HRMS calcd for $\text{C}_{27}\text{H}_{48}\text{NO}_2$ m/z 418.3771 (M^+ + 1), found 418.3679.

Base-Catalyzed Hydrolysis of Compounds 9, 10, and 16. **Compounds 23 and 24.** A solution of 25 mg (0.06 mmol) of compound **9** in 10 mL of 0.6% sodium hydroxide in methanol was heated under reflux for overnight. The solution was carefully acidified with 2 M HCl, and then 6 mL of ethyl ether was added to precipitate the NaCl formed. The solution was filtered, dried over anhydrous sodium sulfate, and evaporated at reduced pressure. The residue was subjected to silica gel (200–240 mesh) column chromatography and eluted with hexane:EtOAc (3:1) to afford compound **23** (3S, 9 mg, 34.7%) as a colorless crystal: mp 144–145 $^\circ\text{C}$; FTIR (neat film) 3400–2500 (br), 2956, 2937, 2869, 2289, 1700, 1464, 1414, 1383, 1289 cm^{-1} ; $^1\text{H NMR}$ (CDCl_3 , 300 Hz) δ 4.20 (m, 1 H), 2.70–2.58 (m, 3 H), 2.44 (dd, $J = 14.3$, 4.4 Hz, 1 H), 2.16–2.03 (m, 1 H), 1.96–1.78 (m, 6 H), 1.25 (s, 3 H), 0.87 (d, $J = 6.6$ Hz, 3 H), 0.85 (d, $J = 6.6$ Hz, 6 H), 0.68 (s, 3 H); $^{13}\text{C NMR}$ (CDCl_3 , 100 MHz) δ 174.1, 116.8, 89.7, 74.4, 55.9, 53.2, 50.6, 42.8, 39.6, 39.5, 39.4, 36.9, 35.9, 35.7, 34.9, 30.2, 28.0, 27.8, 25.6, 24.6, 24.2, 23.7, 22.8, 22.5, 21.2, 18.6, 11.9; FAB MS m/z (relative intensity) 432 (40, M^+ + 1), 414 (M^+ + 1 – H_2O , 100), 396 (M^+ + 1 – $2\text{H}_2\text{O}$, 20); FAB HRMS calcd for $\text{C}_{27}\text{H}_{46}\text{NO}_3$ m/z 432.3478 (M^+ + 1), found 432.3429. Compound **24** was obtained as a mixture of two epimers (13 mg, 37%, 3R:3S = 1:1) as colorless oil: FTIR (neat film) 2951, 2869, 2278, 1725, 1466, 1380, 1281, 1111 cm^{-1} ; $^1\text{H NMR}$ (CDCl_3 , 300 Hz) δ 3.43 (m, 2 H), 3.38 (s, 3 H), 3.37 (s, 3 H), 2.58 (dd, $J = 18.6$, 5.0 Hz, 2 H), 2.53 (m, 4 H), 1.95 (dd, $J = 17.4$, 12.0 Hz, 2 H), 1.32 (s, 3 H), 1.30 (s, 3 H), 0.88 (d, $J = 6.6$ Hz, 6 H), 0.83 (dd, $J = 6.6$ Hz, 12 H), 0.68 (s, 6 H); CI MS m/z (relative intensity) 446 (M^+ + 1, 100), 414 (M^+ + 1 – MeOH, 67), 333 (15), 135 (50), 114 (53); CI HRMS calcd for $\text{C}_{28}\text{H}_{48}\text{NO}_3$ m/z 446.3634 (M^+ + 1), found 446.3641.

Compound 25. A solution of 25 mg (0.06 mmol) of compound **10** in 10 mL of 6% sodium hydroxide in aqueous ethanol was heated under reflux for overnight. The solution was carefully acidified with 2 M HCl until there are white precipitates formed. The solution was extracted with ethyl ether, dried over anhydrous sodium sulfate, and evaporated under pressure. The residue was purified using preparative TLC to afford compound **25** as a mixture of two epimers (17 mg) (3R:3S = 1:1) (61.8%) as colorless oil: FTIR (neat film) 3400–2500 (br), 2926, 2860, 2250, 1700, 1375, 1103, 891; $^1\text{H NMR}$ (CDCl_3 , 300 Hz) δ 4.87 (s, 2 H), 4.79 (s, 2 H), 3.65–3.46

(m, 6 H), 2.52 (d, $J = 6.1$ Hz, 3 H?), 2.33 (dd, $J = 15.9$ Hz, 2 H), 2.12–1.92 (m, 8 H), 1.20 (t, $J = 6.6$ Hz, 6 H), 0.88 (d, $J = 6.6$ Hz, 6 H), 0.83 (d, $J = 6.6$ Hz, 12 H), 0.73 (s, 6 H); EI MS m/z (relative intensity) 459 (M^+ , 10), 441 ($M^+ - H_2O$), 413 ($M^+ - CH_3CH_2OH$), 305 (100); EI HRMS calcd for $C_{29}H_{49}NO_3$ m/z 459.3712, found 459.3700.

Compound 26. A solution of 25 mg (0.06 mmol) of compound **16** in 10 mL of 6% sodium hydroxide in aqueous methanol was heated under reflux for overnight. The solution was carefully acidified with 2 M HCl until there are white precipitates formed. The solution was extracted with ethyl ether, dried over anhydrous sodium sulfate, and evaporated under pressure. The residue was purified using preparative TLC to afford 19 mg of compound **26** (73.0%) as colorless oil: FTIR (neat film) 3400–2500 (br), 2950, 2870, 1733, 1716, 1459, 1382, 1259 cm^{-1} ; 1H NMR ($CDCl_3$, 300 MHz) δ 2.58 (dd, $J = 17.7$, 5.1 Hz, 1 H), 2.35 (t, $J = 7.2$ Hz, 2 H), 2.04 (brd, $J = 12$ Hz, 2 H), 1.95 (dd, $J = 17.7$, 12.0 Hz, 1 H), 1.30 (s, 6 H), 0.90 (d, $J = 6.6$ Hz, 3 H), 0.85 (d, $J = 6.6$ Hz, 6 H), 0.69 (s, 3 H); FAB MS m/z (relative intensity) 435 ($M^+ + 1$, 100), 417 (18), 399 (15), 375 (12), 323 (10); EI HRMS calcd for $C_{27}H_{46}O_4$ m/z 434.3396, found 434.3384.

Alkyl O-Cholestanyl Xanthates (28–32). General procedures for the syntheses of compound **28–32**: potassium *O*-cholestanyl xanthate (**27**)²² (100 mg, 0.20 mmol) was dissolved in 4 mL of warm DMSO, and 1.0 equivalent of alkyl halide was added. After being stirred for 2 h at room temperature, the reaction solution was poured into water and extracted with ethyl acetate. The organic layer was washed with brine and then dried over anhydrous sodium sulfate. After evaporation, the residue was washed with a 5:1 solution of ethyl acetate and petroleum ether to give the corresponding alkyl *O*-cholestanyl xanthate in 80–85% yield. All the xanthates were isolated as amorphous solids. Using bromo acetic acid, compound **28** was obtained as colorless solid: mp 136–138 °C; 1H NMR ($CDCl_3$) δ 5.42 (m, 1 H), 3.88 (s, 2 H), 0.85 (d, $J = 5.4$ Hz, 3 H), 0.83 (d, $J = 6.6$ Hz, 6 H), 0.82 (s, 3 H), 0.62 (s, 3 H); FABMS m/z (relative intensity) 523 ($M^+ + 1$, 5), 506 ($M^+ + 1 - OH$, 3), 464 ($M^+ + 1 - CH_2CO_2H$, 35), 448 ($M^+ + 1 - CH_2CO_2H - CH_4$, 40), 371 ($M^+ + 1 - OC(S)SCH_2CO_2H$, 100). Anal. ($C_{30}H_{50}O_3S_2$) C, H. Using ethyl bromoacetate, compound **29** was obtained as a gum: 1H NMR ($CDCl_3$) δ 5.43 (m, 1 H), 4.18 (q, $J = 7.2$ Hz, 2 H), 3.84 (s, 2 H), 1.26 (t, $J = 7.2$ Hz, 3 H), 0.86 (d, $J = 6.6$ Hz, 3 H), 0.83 (d, $J = 6.6$ Hz, 6 H), 0.82 (s, 3 H), 0.62 (s, 3 H); FABMS m/z (relative intensity) 551 ($M^+ + 1$, 2), 550 (M^+ , 5), 534 ($M^+ - CH_4$, 3), 521 ($M^+ - CH_2CH_3$, 3), 477 ($M^+ - CH_3CH_2OCO$, 5), 463 ($M^+ - CH_3CH_2OCOCH_2$, 5), 371 ($M^+ + 1 - OC(S)SCH_2CO_2Et$, 100). Anal. ($C_{32}H_{54}O_3S_2$) C, H. Using ethyl 2-bromopropionate, compound **30** was obtained as a gum: 1H NMR ($CDCl_3$) δ 5.43 (m, 1 H), 4.28 (q, $J = 7.2$ Hz, 1 H), 4.15 (q, $J = 7.2$ Hz, 2 H), 1.22 (t, $J = 7.2$ Hz, 3 H), 0.85 (d, $J = 6.6$ Hz, 3 H), 0.83 (t, $J = 7.2$ Hz, 3 H), 0.82 (d, $J = 6.6$ Hz, 6 H), 0.81 (s, 3 H), 0.61 (s, 3 H); FABMS m/z (relative intensity) 565 ($M^+ + 1$, 2), 549 ($M^+ + 1 - CH_4$, 5), 520 ($M^+ + 1 - OC_2H_5$, 15), 464 ($M^+ + 1 - CH(CH_3)CO_2Et$, 20), 388 ($M^+ + 1 - C(S)SCH(CH_3)CO_2Et$, 35), 371 ($M^+ + 1 - OC(S)SCH(CH_3)CO_2Et$, 100). Anal. ($C_{33}H_{54}O_3S_2$) C, H. Using ethyl chloroacetate, compound **31** was obtained as a gum: 1H NMR ($CDCl_3$) δ 5.40 (m, 1 H), 4.17 (q, $J = 7.2$ Hz, 2 H), 4.02 (s, 2 H), 3.60 (s, 2 H), 1.25 (t, $J = 7.2$ Hz, 3 H), 0.86 (d, $J = 6.6$ Hz, 3 H), 0.83 (d, $J = 6.6$ Hz, 6 H), 0.81 (s, 3 H), 0.61 (s, 3 H); FABMS m/z (relative intensity) 592 (M^+ , 2), 477 ($M^+ - COCH_2CO_2Et$, 5), 463 ($M^+ - CH_2COCH_2CO_2Et$, 3), 371 ($M^+ + 1 - OC(S)SCH_2COCH_2CO_2Et$, 100). Anal. ($C_{34}H_{56}O_4S_2 \cdot 0.3$ hexane) C, H. Using bromo acetophenone, compound **32** was obtained as a yellowish solid: mp 108–110 °C; 1H NMR ($CDCl_3$) δ 8.00 (m, 2 H), 7.60 (m, 1 H), 7.48 (m, 2 H), 5.42 (m, 1 H), 4.61 (s, 2 H), 0.85 (d, $J = 6.6$ Hz, 3 H), 0.83 (d, $J = 6.6$ Hz, 6 H), 0.78 (s, 3 H), 0.62 (s, 3 H); FABMS m/z (relative intensity) 582 (M^+ , 5), 477 ($M^+ - COC_6H_5$, 5), 463 ($M^+ - CH_2COC_6H_5$, 3), 371 ($M^+ + 1 - OC(S)SCH_2COC_6H_5$, 100). Anal. ($C_{34}H_{56}O_2S_2 \cdot 0.5H_2O$), C, H.

Compound 33. To a solution of 250 mg (0.64 mmol) of cholestan-3-one in 20 mL of methanol was added 6.0 equiv of

4-aminobutyric acid amino acid. The pH was adjusted to 6 by adding glacial acetic acid and then 20 mL of THF, and 1.1 equiv of $NaBH_3CN$ was added. After the mixture was stirred under reflux overnight, 2 M NaOH was added in to a pH of 7. The residue obtained after evaporation was extracted with ethyl acetate, and the organic layer was washed with brine and then dried over anhydrous sodium sulfate. Evaporation gave a residue which was washed with petroleum ether to give compound **33** in 85% yield as an amorphous solid: 1H NMR ($CDCl_3$) δ 3.32 (m, 1 H), 3.05 (m, 2 H), 0.86 (d, $J = 6.0$ Hz, 3 H), 0.83 (d, $J = 7.2$ Hz, 6 H), 0.80 (s, 3 H), 0.62 (s, 3 H); FABMS m/z (relative intensity) 474 ($M^+ + 1$, 100), 430 ($M^+ + 1 - CO_2$, 10), 386 [$M^+ - (CH_2)_3CO_2H$, 10]; FAB HRMS m/z calcd for $C_{31}H_{56}NO_2$ 474.4311 ($M^+ + 1$), found 474.4315.

Compound 34. To a solution of 100 mg (0.27 mmol) of β -cholestanol and cat. $n-Bu_4NI$ in THF was added 1.1 equiv of NaH at room temperature under N_2 . After the mixture was stirred for 1/2 h, 1.0 equiv of bromo acetic acid was added dropwise to the solution. After further stirring for 2 h, 2 M HCl was added to give a pH of 6. The residue obtained after evaporation was extracted with ethyl acetate, and the organic layer was washed with brine and then dried over anhydrous sodium sulfate. After evaporation, the residue was washed with petroleum ether to give compound **34** in 60% yield as colorless solid: mp 169–171 °C (lit.²⁸ 168 °C); 1H NMR ($CDCl_3$) δ 4.11 (s, 1 H), 3.35 (m, 1 H), 0.85 (d, $J = 6.0$ Hz, 3 H), 0.83 (d, $J = 7.2$ Hz, 6 H), 0.77 (s, 3 H), 0.62 (s, 3 H); EIMS m/z (relative intensity) 446 ($M^+ + 1$, 95), 431 (10), 389 (10), 388 (100); FAB HRMS m/z calcd for $C_{29}H_{51}O_3$ 446.3760 ($M^+ + 1$), found 446.3779. Anal. ($C_{29}H_{50}O_3 \cdot 1.2H_2O$), C, H.

Aryl Thiocarbamate and Aryl Carbamate Derivatives of Cholestanol (35–37). General procedure: To a solution of 100 mg (0.27 mmol) of β -cholestanol and cat. $n-Bu_4NI$ in THF was added 1.1 equiv of NaH at room temperature under N_2 . After the mixture was stirred for 1/2 h, 1.0 equiv of isothiocyanate or isocyanate was added dropwise. After the mixture was stirred for 2 h, the residue obtained by evaporation was extracted with ethyl acetate, and the organic layer was washed with brine and dried over anhydrous sodium sulfate. Evaporation gave a residue that was washed with petroleum ether to yield compounds **35–37** in 75–80% yield. Using phenyl isothiocyanate, compound **35** was obtained as yellowish crystals: mp 176–178 °C (lit.²⁹ 180–181 °C); 1H NMR ($CDCl_3$) δ 7.32 (m, 4 H), 7.22 (m, 1 H), 5.30 (m, 1 H), 0.85 (d, $J = 6.0$ Hz, 3 H), 0.83 (d, $J = 7.2$ Hz, 6 H), 0.77 (s, 3 H), 0.62 (s, 3 H); FABMS m/z (relative intensity) 524 ($M^+ + 1$, 5), 388 [$M^+ + 1 - C(S)NHPH$, 4], 371 [$M^+ + 1 - OC(S)NHPH$, 100]; FAB HRMS m/z calcd for $C_{34}H_{54}NOS$ ($M^+ + 1$) 524.3926, found 524.3884. Anal. ($C_{34}H_{53}NOS \cdot 2H_2O$), C, N; H: calcd, 10.26; found 9.68.

Using 1-naphthyl isothiocyanate, compound **36** was obtained as yellowish crystals: mp 137–139 °C; 1H NMR ($CDCl_3$) δ 7.87 (m, 4 H), 7.52 (m, 3 H), 5.31 (m, 1 H), 0.87 (d, $J = 6.0$ Hz, 3 H), 0.85 (d, $J = 6.6$ Hz, 6 H), 0.84 (s, 3 H), 0.62 (s, 3 H); FABMS m/z (relative intensity) 574 ($M^+ + 1$, 60), 388 [$M^+ + 1 - C(S)NHNaphth$, 10], 371 [$M^+ + 1 - OC(S)NHNaphth$, 100]; HRMS (FAB) m/z calcd for $C_{38}H_{56}NOS$ 574.4083 ($M^+ + 1$), found 524.4111. Anal. ($C_{38}H_{55}NOS \cdot 1.6H_2O$), C, N; H: calcd 9.73; found 9.30. Using phenyl isocyanate, compound **37** was obtained as yellowish crystals: 146–148 °C (lit.³⁰ 151 °C); 1H NMR ($CDCl_3$) δ 7.32 (m, 4 H), 7.04 (m, 1 H), 4.66 (m, 1 H), 0.87 (d, $J = 6.0$ Hz, 3 H), 0.83 (d, $J = 6.6$ Hz, 6 H), 0.80 (s, 3 H), 0.62 (s, 3 H); FABMS m/z (relative intensity) 508 ($M^+ + 1$, 30), 428 (100), 371 ($M^+ + 1 - O_2CNHPH$, 95); FAB HRMS m/z calcd for $C_{34}H_{54}NO_2$ 508.4155 ($M^+ + 1$), found 508.4149. Anal. ($C_{34}H_{53}NO_2 \cdot 0.25H_2O$), C, H, N.

X-ray Analysis. Detailed crystal data and summaries of data collection and structure refinement for compounds **4**, **8**, and **13** are listed in Table 12 in the Supporting Information. Crystals of compound **4** were obtained by slow evaporation from a mixture of hexanes–ethyl acetate (10:1). Compound **4** was crystallized in space group $P2_1$ with $a = 11.0952(10)$ Å, $\alpha = 90^\circ$, $b = 6.4084(6)$ Å, $\beta = 103.5220^\circ$, $c = 18.121(2)$ Å, $\gamma = 90^\circ$, and it was refined to a conventional factor $R = 0.0547$

and goodness of fit on $F^{\wedge}2 = 1.024$. Data collection was at 173 K, with $Z = 2$. The structure of compound **4** is shown in Figure 2.

Crystals of compound **8** were obtained by slow evaporation from a chloroform solution. Compound **8** was crystallized orthorhombic in space group $P2_12_12_1$ with $a = 6.4670(2)$ Å, $b = 34.1026(12)$ Å, $c = 35.4789(13)$ Å and refined to a conventional factor $R = 0.0690$ and goodness of fit on $F^{\wedge}2 = 1.086$. Data collection was at 248 K, with $Z = 12$; The structure of compound **8** is shown in Figure 3.

Crystals of compound **13** were obtained by slow evaporation from hexanes–ethyl acetate (1:1). Compound **13** was crystallized orthorhombic in space group $P2_12_12_1$ with $a = 6.2731(6)$ Å, $\alpha = 90^\circ$, $b = 9.8150(9)$ Å, $\beta = 90^\circ$, $c = 40.038(4)$ Å, $\gamma = 90^\circ$, and it was refined to a conventional factor $R = 0.0758$ and goodness of fit on $F^{\wedge}2 = 0.993$. Data collection was at 233 K, with $Z = 4$. The structure of compound **13** is shown in Figure 4.

Expression and Purification of the Cytoplasmic Region of CD45. The cytoplasmic region of CD45, fused at the C-terminal to six histidines, was expressed in the pET23D vector (Novagen). The 705 amino acids of CD45 being expressed begins MAGNLDEQQELV and ends ALNQGSHHH-HHH and has a molecular weight of 83,664. *Escherichia coli* BL21 (DE3) transformed with the expression plasmid was grown in a 10 L fermentor at 28 °C to an optical density at 600 nm of 0.6 and induced by the addition of 0.6 g of IPTG (isopropyl- β -thiogalactopyranoside). After 5 h the cells were harvested by centrifugation and stored at -80°C . The CD45 was purified by metal affinity and gel filtration chromatography. Briefly, cells were lysed by two passes through a French pressure cell at 16 000 psi, and the lysate clarified by centrifugation at 47000g for 60 min at 4 °C. The supernatant was applied to a 50 mL Chelating Sepharose Fast Flow (Pharmacia) column charged with NiCl_2 and equilibrated in 25 mM Hepes, 250 mM NaCl and 25 mM imidazole at pH 7.5. The column was eluted with a linear gradient from 25 to 250 mM imidazole. Fractions containing CD45 phosphatase activity (50–100 mM imidazole fractions) were pooled and concentrated with a Centrprep 30 (Amicon). The concentrate was applied to a 2 L Superdex 75 (Pharmacia) column equilibrated in 20 mM Tris and 100 mM NaCl at pH 8.0. Fractions containing CD45 phosphatase activity were pooled (approximately 80% pure), aliquoted, and stored at -80°C .

Cdc25A Inhibition Assay. The procedures for the preparation of GST-Cdc25A fusion protein and Cdc25A inhibition assay have been described in detail previously.²² Briefly, each batch of GST-Cdc25A fusion protein was calibrated such that the quantity added to each well dephosphorylated FDP in a linear fashion over a 20 min reaction time course in the preliminary study. The phosphatase assay was performed in 96-well plates. The standard reaction time and conditions were 15 min at 25 °C in a darkened chamber. The reactions were terminated with 15 μL of sodium orthovanadate (285 mM) dissolved in distilled water. The fluorescence emission of the reaction product (fluorescein monophosphate) was measured with a Millipore Cytofluor 2350 fluorimeter (excitation wavelength, 485 nm; emission wavelength, 530 nm). The IC_{50} values were determined from at least two independent determinations, each run in triplicate, where the variation from the mean did not exceed $\pm 20\%$.

Assays for Cdc25A kinetic study were performed in duplicate in 96-well plates with 3-*O*-methylfluorescein phosphate (U.S. Biochemicals) as substrate at the indicated final concentrations in a final volume of 100 μL of assay buffer consisting of 50 mM HEPES, 1 mM EDTA, and 1 mM dithiothreitol (pH 7.4). Cdc25 enzyme was diluted to ~ 50 nM. Inhibitors were dissolved in DMSO and comprised 5 μL of the final assay volume. Excitation wavelength was 485 nm, emission was monitored at 530 nm on a PerSeptive Biosystems Cytofluor, and readings were taken at 1 min intervals for 10 min to ensure linearity. Relative fluorescence units from the 5 min reading were fit to the Michaelis–Menten equation in Excel.

CD45 Inhibition Assay and Steady-State Kinetics. CD45 assays in triplicate were performed with *p*-nitrophenyl phosphate as substrate in 96-well plates at 25 °C in a final volume of 100 μL using 10 ng of enzyme. Assay buffer was composed of 50 mM HEPES, 100 mM NaCl, and 2 mM dithiothreitol, pH 7.4. Compound **17** was added to the wells dissolved in 5 μL of DMSO at a final concentration of 5, 10, or 15 μM , followed by 20 μL of enzyme and 75 μL of *p*NPP substrate. Substrate concentration was varied between 5 and 30 μM ($K_m = 15$ μM). Absorbance at 405 nm was monitored for 30 min, and reaction rates under linear conditions were determined using Molecular Devices SOFTmax Pro. Under these conditions, inhibition of CD45 by compound **17** appeared to be mostly noncompetitive but having a mixed component as indicated by the intersection above the x axis.

Cytotoxicity Assays. The in vitro cytotoxicity assays were carried out at the National Cancer Institute. Details of the assay procedures have been reported previously.²⁵

Acknowledgment. We gratefully acknowledge support of this research by the NCI/NIH (5U19-CA52995). We are grateful to Dr. Donald G. VanDerveer and Dr. Leslie T. Gelbaum for their valuable assistance in obtaining single crystal X-ray and high resolution NMR data. We thank Mr. David E. Bostwick and Ms. Sarah J. Shealy for mass spectroscopic services.

Supporting Information Available: Atomic coordinate information for compounds **4**, **9**, and **13**. This material is available free of charge via the Internet at <http://pubs.acs.org>.

References

- (1) A preliminary account of this work has been presented: Peng, H.; Zalkow, L. H.; Abraham, R. T.; Powis, G. Novel CDC25A Phosphatase Inhibitors from Pyrolysis of 3- α -Azido-B-homo-6-oxa-4-cholesten-7-one on Silica Gel. *J. Med. Chem.* **1998**, *41*, 4677–4680.
- (2) (a) Barford, D.; Das, A. K.; Ggloff, M. P. The structure and mechanism of protein phosphatase: insight into catalysis and regulation. *Annu. Rev. Biophys. Biomol. Struct.* **1998**, *27*, 133–164. (b) Zhang, Z.-Y. Protein-tyrosine phosphatases: biological function, structural characteristics, and mechanism of catalysis. *Crit. Rev. Biochem. Mol. Biol.* **1998**, *33*, 1–52.
- (3) (a) Millar, J. B.; Blevitt, J.; Gerace, L.; Sadhu, K.; Featherstone, C.; Russell, P. p55^{CDC25} is a nuclear protein required for the initiation of mitosis in human cells. *Proc. Natl. Acad. Sci. U.S.A.* **1991**, *88*, 10800–10504. (b) Lammer, C.; Wagerer, S.; Saffrich, R.; Mertens, D.; Ansorge, W.; Hoffmann, I. The cdc25B phosphatase is essential for the G2/M phase transition in human cells. *J. Cell Sci.* **1998**, *111*, 2445–2453.
- (4) (a) Sanchez, Y.; Wong, C.; Thoma, R. S.; Richman, R.; Wu, Z.; Piwnicka-Worms, H.; Elledge, S. J. Conservation of the Chk1 checkpoint pathway in Mammals: linkage of DNA damage to cdk regulation through cdc25. *Science* **1997**, *277*, 1497–1501. (b) Lopez-Girona, A.; Furnari, B.; Odile, M.; Russell, P. Nuclear localization of Cdc25 is regulated by DNA damage and a 14-3-3 protein. *Nature* **1999**, *397*, 172–175.
- (5) (a) Jinno, S.; Suto, K.; Nagata, A.; Igrashi, M.; Kanaoka, Y.; Nojima, H.; Okayama, H. Cdc25A is a novel phosphatase functioning early in the cell cycle. *EMBO J.* **1994**, *13*, 1549–1556. (b) Hoffmann, I.; Draetta, G.; Karsenti, E.; Activation of the phosphatase activity of human cdc25A by a cdk2-cyclin E dependent phosphorylation at the G1/S transition *EMBO J.* **1994**, *13*, 4302–4310.
- (6) (a) Gasparotto, D.; Maestro, R.; Piccinin, S.; Vukosavljevic, T.; Barzan, L.; Sulfaro, S.; Boiocchi M. Overexpression of CDC25A and CDC25B in head and neck cancers. *Cancer Res.* **1997**, *57*, 2366–2368. (b) Kudo, Y.; Yasui, W.; Ue, T.; Yamamoto, S.; Yokozaki, H.; Nikai, H.; Tahara, E. Overexpression of cyclin-dependent kinase-activating CDC25B phosphatase in human gastric carcinomas. *Jpn. J. Cancer Res.* **1997**, *88*, 9947–9952. (c) Wu, W.; Fan, Y. H.; Kemp, B. L.; Walsh, G.; Mao, L. Overexpression of cdc25A and cdc25B is frequent in primary non-small cell lung cancer but is not associated with overexpression of c-myc. *Cancer Res.* **1998**, *58*, 4082–4085. (d) Dixon, D.; Moyana, T.; King, M. J. Elevated expression of cdc25A protein phosphatase in colon cancer. *Exp. Cell Res.* **1998**, *240*, 236–243. (e) Hernandez, S.; Hernandez L.; Bea, S.; Cazorla, M.; Fernandez, P. L.; Nadal, A.; Muntane, J.; Mallofre, C.; Monterrat, E.; Cardesa, A.; Campo, E. Cdc25 cell cycle-activating phosphatase and c-Myc expression in human non-Hodgkin's lymphoma *Cancer Res.* **1998**, *58*, 1762–1767.

- (7) (a) Galaktionov, K.; Lee, A. K.; Eckstein, J.; Draetta, G.; Meckler, J.; Loda, M.; Beach, D. CDC25 phosphatases as potential human oncogenes. *Science* **1995**, *269*, 1575–1577. (b) Galaktionov, K.; Chen, X.; Beach, D. Cdc25 cell-cycle phosphatase as a target of c-myc. *Nature* **1996**, *382*, 511–517. (c) Galaktionov, K.; Jessus, C.; Beach, D. Raf1 interaction with Cdc25 phosphatase ties mitogenic signal transduction to cell cycle activation. *Genes Dev.* **1996**, *9*, 1046–1058.
- (8) Draetta, G.; Eckstein, J. Cdc25 protein phosphatases in cell proliferation. *Biochim. Biophys. Acta* **1997**, *1332*, M53–62.
- (9) (a) Sheppeck, J. E.; Gauss, C. M.; Chamberlin, A. R. Inhibition of the Ser-Thr phosphatases PP1 and PP2A by naturally occurring toxins. *Bioorg. Med. Chem.* **1997**, *5*, 1739–1750. (b) Gupta, V.; Ogawa, A. K.; Du, X.; Houk, K. N.; Armstrong, R. W. A model for binding of structurally diverse natural product inhibitors of protein phosphatases PP1 and PP2A. *J. Med. Chem.* **1997**, *40*, 3199–3206.
- (10) Baratte, B.; Meijer, L.; Galaktionov, K.; Beach, D. Screening for antimetabolic compounds using the cdc25 tyrosine phosphatase, an activator of the mitosis-inducing p34^{cdc2}/cyclin B^{cdc13} protein kinase. *Anticancer Res.* **1992**, *12*, 873–880.
- (11) (a) Gunasekera, S. P.; McCarthy, P. J.; Kelly-Broger, M.; Lobkovsky, E.; Clardy, J. Dysidiolide: A novel protein phosphatase inhibitor from Caribbean Sponge *Diysidea ehteria* de Laubenfels. *J. Am. Chem. Soc.* **1996**, *118*, 8759–8760. (b) Blanchard, J. L.; Epstein, D. M.; Boisclair, M. D.; Rudolph, J.; Pal, K. Dysidiolide and related gamma-hydroxy butenolide compounds as inhibitors of the protein tyrosine phosphatase, CDC25. *Bioorg. Med. Chem. Lett.* **1999**, *9*, 2537–2538.
- (12) Cebula, R. E.; Blanchard, J. L.; Boisclair, M. D.; Pal, K.; Bockovich, N. J. Synthesis and phosphatase inhibitory activity of analogues of Sulfircin. *Bioorg. Med. Chem. Lett.* **1997**, *7*, 2015–2020.
- (13) (a) Ham, S. W.; Park, H. J.; Lim, D. H. Studies on Menadione as an inhibitor of the cdc25 phosphatase. *Bioorg. Chem.* **1997**, *25*, 33–36. (b) Ham, S. W.; Park, J.; Lee, S.; Kim, W.; Kang, K.; Choi, K. H. Naphthoquinone analogues as inactivator of cdc25 phosphatase. *Bioorg. Med. Chem. Lett.* **1998**, *8*, 2507.
- (14) Rice, R. L.; Rusnak, J. M.; Yokokawa, F.; Yokokawa, S.; Messner, D.; Boynton, A. L.; Wipf, P.; Lazo, J. S. A targeted library of small-molecule, tyrosine, and dual-specificity phosphatase inhibitors from a rational core design and random side chain variation. *Biochemistry* **1997**, *36*, 15965.
- (15) Bergnes, G.; Gilliam, C. L.; Boisclair, M. D.; Blanchard, J. L.; Blake, K. V.; Epstein, D. M.; Pal, K. Generation of an Ugi library of phosphate mimic-containing compounds and identification of novel dual specific phosphate inhibitors. *Bioorg. Med. Chem. Lett.* **1999**, *9*, 2849–2854.
- (16) Hill, R. K.; Conley, R. T.; Chortyk, O. T. Beckmann rearrangement in strong acid. *J. Am. Chem. Soc.* **1965**, *87*, 5646–5651.
- (17) Barton, D.; Ollis, W. D.; et al. *Comprehensive Organic Chemistry, the Synthesis of Organic Compounds*; Pergamon Press: New York, 1979; Vol. 2, pp 968–970.
- (18) (a) Zook, H. D.; Pavlak, S. C. Fission of *tert*-butyl alkyl ketone in Schmidt reaction. *J. Am. Chem. Soc.*, **1955**, *77*, 2501–2503. (b) Conley, R. T.; Nowak, B. E. Schmidt reaction in polyphosphoric acid. II Abnormal rearrangements of ketones. *J. Org. Chem.* **1961**, *26*, 692–696. (c) Barton, D. H. R. Campos-Neves, A. da. S.; Scott, A. I. An approach to the partial synthesis of aldosterone from steroids lacking substitution at C₁₈. *J. Chem. Soc.* **1957**, 2698–2706.
- (19) (a) Rodewald, W. J.; Achmatowicz, B. The second-order Beckmann rearrangement of steroidal oximes. *Roczniki Chem.* **1972**, *46*, 203–208. (b) Suginome, H.; Furukawa, K.; Orito, K. Nitrogen insertion to bicyclo[2.2.1] heptanones – the photo-Beckmann rearrangement of oximes of (+)-fenchone and (+)-camphor. *J. Chem. Soc., Chem. Commun.* **1987**, 1004. (c) Lansbury, P. T.; Mazur, D. J.; Springer, J. P. Total synthesis of pseudoguianolide 4. A stereoselective approach to baldulin. *J. Org. Chem.* **1985**, *50*, 1632.
- (20) Lettre, H.; Mathes, K.; Wagner, M. Improved Synthesis of 6-aza-steroid. *Liebigs Ann. Chem.* **1967**, *703*, 147–151.
- (21) Ritter, J. J.; Minieri, P. P. A new reaction of nitriles. I. Amides from alkenes and mononitriles. *J. Am. Chem. Soc.* **1948**, *70*, 4045–4048.
- (22) Peng, H.; Xie, W.; Kim, D. I.; Zalkow, L. H.; Powis, G.; Otterness, D. M.; Abraham, R. T. Steroidal derived acid as inhibitors of human Cdc25A protein phosphatase. *Bioorg. Med. Chem.* **2000**, *8*, 299–306.
- (23) (a) Trowbridge, I. S. CD45, A prototype for transmembrane protein tyrosine phosphatases. *J. Biol. Chem.* **1991**, *1095*, 46–56. (b) Justement, L. B. The role of CD45 in signal transduction. *Adv. Immunol.* **1997**, *66*, 1–65.
- (24) Boyd, M. R. The NCI in vitro anticancer drug discovery screen: concept, implementation, and operation. In *Anticancer drug development guide: preclinical screening, clinical trials, and approval*; Teicher, B. A., Ed.; Humana Press: Totowa, 1997; pp 23–56.
- (25) Monks, A.; Scudiero, D.; Skehan, P.; Shoemaker, R.; Paull, K.; Vistica, D.; Hose, C.; Langley, J.; Cronise, P.; Vaigro-Wolff, A.; Gray-Goodrich, M.; Campbell, H.; Mayo, J.; Boyd, M. Feasibility of a high-flux anticancer drug screen using a diverse panel of cultured human tumor cell lines. *J. Natl. Cancer Inst.* **1991**, *83*, 757–766.
- (26) Dauben, W. G.; Fonken, G. J. Reactions of B-norcholesterol. *J. Am. Chem. Soc.* **1956**, *78*, 4736–4743.
- (27) Scherm, A.; Hummel, Arthur. US Patent 4,602,037, 1986.
- (28) Ahmad, M. S.; Logani, S. C.; LiAlH₄–AlCl₃ reduction of steroidal cyclic acetals. *Aust. J. Chem.* **1971**, *24*, 143–151.
- (29) Heath-Brown, B.; Heilbron, I. M.; Jones, E. R. Studies in the sterol group. Part XLII. The constitution of zymosterol. *J. Chem. Soc.* **1940**, 1482–1489.
- (30) Barton, D. H. R.; Fontana, G.; Yand, Y.; The invention free radical reactions. Part XXXV. A novel radical fission reaction of N-sulfonylthiocarbamates. *Tetrahedron* **1996**, *52*, 2705–2716.
- (31) Taing, M.; Keng, Y.-F.; Shen, K.; Wu, L.; Lawrence, D. S.; Zhang, Z.-H. Potent and highly selective inhibitors of the protein tyrosine phosphatase 1B. *Biochemistry* **1999**, *38*, 3793–3803.

JM0004401